FINAL REPORT

Chemical Decomposition Combined with Physical Adsorption for the Treatment of Investigation-Derived Waste Containing PFAS

SERDP Project ER18-1482

MAY 2020

Hyeok Choi
The University of Texas at Arlington

SERDP
DOD ▪ EPA ▪ DOE

Page Intentionally Left Blank

Page Intentionally Left Blank

REPORT DOCUMENTATION PAGE

Form Approved
OMB No. 0704-0188

1. REPORT DATE *(DD-MM-YYYY)*	**2. REPORT TYPE**	**3. DATES COVERED** *(From - To)*
05-01-2020	SERDP Final Report	Sep 2018 – May 2020

4. TITLE AND SUBTITLE

(Limited Scope) Chemical Decomposition Combined with Physical Adsorption for the Treatment of Investigation-Derived Waste Containing PFAS

5a. CONTRACT NUMBER
W912HQ18P0091

5b. GRANT NUMBER

5c. PROGRAM ELEMENT NUMBER

6. AUTHOR(S) Hyeok Choi, Ph.D.; Junha Jeon, Ph.D.

5d. PROJECT NUMBER
ER18-1482

5e. TASK NUMBER

5f. WORK UNIT NUMBER

7. PERFORMING ORGANIZATION NAME(S) AND ADDRESS(ES)
The University of Texas at Arlington
701 S. Nedderman Dr.
Arlington, TX 76019, USA

8. PERFORMING ORGANIZATION REPORT NUMBER
1260401650

9. SPONSORING / MONITORING AGENCY NAME(S) AND ADDRESS(ES)

Strategic Environmental Research and Development Program
4800 Mark Center Drive, Suite 16F16
Alexandria, VA 22350-3605

10. SPONSOR/MONITOR'S ACRONYM(S)
SERDP

11. SPONSOR/MONITOR'S REPORT NUMBER(S) ER18-1482

12. DISTRIBUTION / AVAILABILITY STATEMENT
DISTRIBUTION STATEMENT A. Approved for public release: distribution unlimited.

13. SUPPLEMENTARY NOTES

14. ABSTRACT

Considering the Agency's emphasis on development of destructive technologies for treatment of per- and polyfluoroalkyl substances (PFAS) in investigation-derived waste and the current need of treatment train approaches, the objective was to integrate various treatment technologies into one engineered system to synergistically remove and decompose PFAS. Adsorption-mediated chemical oxidation integrated with chemical reduction was proposed. Transition metals in any forms were conjugated with common oxidants such as persulfate to generate various oxidizing and reducing species through the established Fenton-like reaction. The chemical decomposition of PFAS was also combined with their physical adsorption by utilizing transition metal particles impregnated into the mesoporous structure of granular activated carbon. Results showed the modified Fenton system is effective to remove PFAS. Chemical oxidants conjugated with transition metals were able to decompose PFAS, particularly carboxylic PFAS, under ambient conditions. Sulfonic PFAS were removed mainly via adsorption mechanism, while remaining undecomposed. This study made us one step-closer to achieving our objective and study target, i.e., integrated destructive system based on practical technologies. The most practical Fenton reaction and its modifications should be revisited to address treatment of complex media contaminated with PFAS.

15. SUBJECT TERMS
Per- and Ploy fluoroalkyl Substances (PFAS); Investigation-Derived Waste (IDW); Treatment and Remediation; Advanced Oxidation and Reductive Decomposition; Adsorption; Fenton-like Reaction

16. SECURITY CLASSIFICATION OF:			**17. LIMITATION OF ABSTRACT**	**18. NUMBER OF PAGES**	**19a. NAME OF RESPONSIBLE PERSON**
a. REPORT	**b. ABSTRACT**	**c. THIS PAGE**			Hyeok Choi, Ph.D.
U	U	U	UU	53	**19b. TELEPHONE NUMBER** *(include area code)* 817-272-5116

Page Intentionally Left Blank

Table of Contents

List of Tables

List of Figures

List of Acronyms

6:2 FTS	6:2 fluorotelomer sulfonate
Ag; Ag^0; Ag^+	Silver
AOTs	Advanced oxidation technologies
Au	Gold
Co; Co^{2+}	Cobalt
Cu	Copper
Def-PFAS	Defluorinated per- and polyfluoroalkyl substances
e^-	Electrons
ERSON	Statements of need
F^-	Fluoride ion
Fe; Fe^0; Fe^{2+}; Fe^{3+}	Iron
Fe_2O_3; FeO	Iron oxide
GAC	Granular activated carbon
H_2	Hydrogen
Halo-POCs	Halogenated persistent organic chemicals
HP; H_2O_2	Hydrogen peroxide
HRs	Hydroxyl radicals
IDW	Investigation-derived waste
Ir	Iridium
LC	Liquid chromatograph
M; M^x; M^0	Transition metal
MeOH	Methanol
MO_x	Transition metal oxide
MS	Mass spectrometer
Ni	Nickel
PFAS	Per- and polyfluoroalkyl substances
PFBA	Perfluorobutanoic acid
PFBS	Perfluorobutanesulfonic acid
PFHpA	Perfluoroheptanoic acid
PFHxA	Perfluorohexanoic acid
PFHxS	Perfluorohexanesulfonic acid
PFNA	Perfluorononanoic acid
PFOA	Perfluorooctanoic acid
PFOS	Perfluorooctanesulfonic acid
PFPeA	Perfluoropentanoic acid
PMS; HSO_5^-	**P**eroxymonosulfate
POCs	Persistent organic chemicals
PS; $S_2O_8^{2-}$	Persulfate
RAC; GAC/M; GAC/Fe^0	Reactive activated carbon

RNIP	Reactive nanoscale iron particle
SRAs; $O_2^{\bullet-}$	Superoxide radical anions
SRs	Sulfate radicals
TBA	Tert-butyl alcohol
TOC	Total organic carbon
UCMR-3	3rd Uncontrolled Contaminant Monitoring Rule
ZVI; Fe^0	Zerovalent iron

Keywords

Per- and Polyfluoroalkyl Substances; Perfluorooctanoic Acid; Perfluorooctanesulfonic Acid; Investigation-derived Waste; Treatment and Remediation

Physical Adsorption; Advanced Oxidation; Reductive Decomposition

Granular Activated Carbon; Reactive Activated Carbon; Chemical Oxidants; Transition Metals; Fenton-like Reaction; Zerovalent Iron; Radical Mechanisms

Integrated System; Destructive and Practical Technologies; Ambient Conditions; Complex Media

Acknowledgements

This research was fully supported by the Department of Defense through the Strategic Environmental Research and Development Program (ER18-1482). We also acknowledge Cabot Norit Americas for kindly donating the GAC.

Abstract

Introduction and Objective: Considering the emphasis of the Environmental Restoration Statements of Need on *easily deployable and destructive technologies* for treatment of per- and polyfluoroalkyl substances (PFAS) in investigation-derived waste (IDW) and the current need of *treatment train approaches*, the overall objective is to integrate various treatment technologies into one engineered system to synergistically remove and decompose PFAS. In doing so, our study target is set that such an integrated system should be based on *practical technologies, if possible, working under ambient conditions*, which is highly challenging but significant.

Technical Approach: Adsorption-mediated advanced oxidation integrated with chemical reduction is proposed. Transition metals (M) in any forms, e.g., zerovalent iron nanoparticles (Fe^0) and dissolved silver ions (Ag^+), are conjugated with common oxidants such as persulfate (PS) and hydrogen peroxide. Various reactive species over reaction conditions, including electrons (e^-), hydrogens (H_2), and superoxide radical anions (SRAs) as reductants as well as hydroxyl radicals (HRs) and sulfate radicals (SRs) as oxidants, can be generated through the Fenton-like reaction. Chemical decomposition of PFAS can also be optionally combined with their physical adsorption by utilizing transition metal particles (M^0/MO_x) impregnated into the mesoporous structure of granular activated carbon (GAC), so-called reactive activated carbon (RAC; GAC/M).

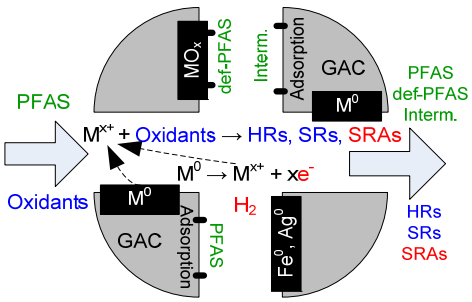

Results: This limited scope project tested proof of the concept to determine whether the integrated system, i.e., RAC/oxidant or M/oxidant, is effective to adsorb and decompose PFAS. In particular, the modified Fenton system was quickly evaluated for its capability to decompose PFAS. Batch experiments were conducted to investigate the effects of GAC, oxidant, metal, dose, pH, and temperature on the removal of mainly 6 PFAS (all perfluorinated ones) listed in the United States Environmental Protection Agency's 3rd Uncontrolled Contaminant Monitoring Rule. Results showed that the integrated system is effective to remove PFAS via physical adsorption and/or chemical decomposition. Chemical oxidants conjugated with transition metals (e.g., PS/Ag pair) were able to decompose PFAS, particularly carboxylic PFAS, under ambient conditions. Sulfonic PFAS were removed mainly via adsorption mechanism, while remaining undecomposed under the tested conditions. As a polyfluorinated one, 6:2 fluorotelomer sulfonate was also decomposed significantly even by PS alone at room temperature. The most practical Fenton reaction and its modifications should be revisited to better address treatment of complex media contaminated with PFAS.

Benefits: This study made us one step-closer to achieving our objective and study target, i.e., integrated destructive system based on practical technologies, as a new research direction. Along with revealing detailed PFAS decomposition mechanisms and pathways as well as fate and transport of PFAS in IDW, future research should be set toward accelerating decomposition of PFAS in the promising Fenton system by pairing other common oxidants and transition metals at/in different oxidation states/elemental groups and introducing new approaches to tackle sulfonic PFAS such as Ag-PS complex utilization and catalytic substitution reaction. Knowledge obtained from this study could be expanded to treat many other halogenated chemicals (e.g., short-chain PFAS) found in various real-world complex media. We envision ultimate treatment procedure later would be mainly simple mixing of IDW with RAC/oxidant or M/oxidant.

Executive Summary

Objective

This study addresses the objective of the Statements of Need (ERSON-18-L1) to develop innovative approaches for treatment of per- and polyfluoroalkyl substances (PFAS) in complex media such as investigation-derived waste (IDW). Considering the emphasis of the SON on *easily deployable and destructive technologies* and the current need of *treatment train approaches*, the overall objective is to integrate various treatment technologies into one engineered system to synergistically remove and decompose the most challenging PFAS. In doing so, our study target is set that such an integrated system should be based on *practical technologies, if possible, working under ambient conditions*, which is challenging but significant. We propose adsorption-mediated advanced oxidation integrated with chemical reduction.

Transition metals (M; M^x, x=0~+3) in any forms (i.e., solid particles/dissolved ions, zerovalent/oxidized ones), including zerovalent iron nanoparticles (Fe^0; ZVI) and dissolved silver ions (Ag^+), are conjugated with common oxidants such as hydrogen peroxide (HP; H_2O_2). peroxymonosulfate (PMS; HSO_5^-), and persulfate (PS; $S_2O_8^{2-}$). Various reactive species, including electrons (e^-), hydrogens (H_2), and superoxide radical anions (SRAs; $O_2^{\bullet-}$) as reductants and hydroxyl radicals (HRs; $^{\bullet}OH$) and sulfate radicals (SRs; $SO_4^{\bullet-}$) as oxidants, can be generated through the established Fenton-like reaction. Combining advanced oxidation with chemical reduction can harness the two complementary treatment approaches and thus leverage various PFAS decomposition pathways. Chemical decomposition of PFAS can also be combined with their physical adsorption by embedding metal particles (M^0/MO_x) into the mesoporous structure of granular activated carbon (GAC), namely reactive activated carbon (RAC; GAC/M).

As a result, this limited scope project promptly tests proof of the concept to determine whether the integrated system (RAC/oxidants or M/oxidants) is effective to physically adsorb and chemically decompose PFAS. In particular, the modified Fenton system should be evaluated for essential data acquisition because previous studies pointed out that even the most powerful and practical Fenton reaction is not effective to decompose PFAS [1,2]. If successful, IDW and other complex media can be simply mixed with RAC/oxidants or M/oxidants for their treatment under ambient conditions. We respond to the emphases of the ERSON by proposing and testing the destructive technology potentially characterized with high treatment effectiveness, flexible treatment scheme, and easily deployable feature.

Background

PFAS and IDW: PFAS are highly persistent organic chemicals (POCs). Perfluorooctanoic acid (PFOA) and perfluorooctanesulfonic acid (PFOS), the two most widely used PFAS have been the recent focus of US federal regulation. Due to their unique properties, PFAS have been useful in manufacturing many industrial and military products (e.g., aqueous film-forming foams). Once released, they are not (or rarely) decomposed in either natural environments or treatment facilities. Particularly, treatment of PFAS in IDW like many other complex media is challenging because IDW consists of various heterogenous components. The ERSON indicates that destructive technologies are preferred to avoid future environmental liability issues. Technologies should also have the potential for on-site applications.

Destructive technologies-advanced oxidation: Attention has been given to advanced oxidation technologies (AOTs), which utilize strong transient oxidizing species such as HRs and SRs. Among many AOTs, radicals can be "practically generated under ambient conditions" via

activation of common oxidants (e.g., HP, PS, and PMS) with transition metals (M) such as Fe, Ag, and cobalt (Co), known as the Fenton-like reaction [3,4]. However, the most established Fenton reaction proven to decompose and mineralize a variety of POCs has been reported to be less effective for PFAS due to the extraordinarily strong C−F bonds in PFAS [1,2]. Thus, research studies involving AOTs for PFAS decomposition introduce other working mechanisms such as photolysis, along with HRs and SRs mechanisms. They include H_2O_2/UV photo-Fenton, TiO_2/UV photocatalysis, and sonochemical processes for HRs generation as well as $S_2O_8^{2-}$/UV, HSO_5^-/UV, and $S_2O_8^{2-}$/microwave for SRs generation [1,2,5]. Heat-activated PS has also shown decomposition of PFAS [5]. In spite of their effectiveness, these technologies commonly require energy-intensive tools such as UV, ultrasound, microwave, electron beam, and high temperature.

Destructive technologies-chemical reduction: Chemical reduction or reductive dehalogenation has been proposed to treat halogenated-POCs (halo-POCs). Use of metal nanoparticles in zerovalent state (M^0), such as Fe^0, has been most known. While M^0 oxidizes, it provides electrons for dehalogenation of halo-POCs [6]. Although reductive defluorination of PFAS by Fe^0 is thermodynamically feasible, successful defluorination has been scarcely reported. Even if occurring, final products will be defluorinated PFAS (def-PFAS), and thus mineralization of PFAS by the reductive pathway is hard to expect, unlike AOTs. However, def-PFAS become more vulnerable to decomposition by subsequent oxidation processes. In addition, metal particles (M^0 and MO_x) are also known to remove PFAS via adsorption or complexation.

Proposed treatment strategy: Considering the advantages of the two complementary chemical approaches and their limitations mentioned above, we propose to exploit an engineered system which combines AOTs with chemical reduction methods. Transition metals in any forms (M) are coupled with common oxidants. Specifically, when Fe^0 interacts with HP, Fe^0 releases Fe ions during (if any) reductive decomposition of PFAS and then Fe ions can activate HP to generate HRs. Fe^0 can also be coupled with many other oxidants. When conjugated with PS and PMS, mostly SRs are generated. Interestingly, HP at high concentrations coupled with Fe has been reported to trigger a catalytic HP propagation reaction to produce various reactive radicals including HRs, SRs, and particularly SRAs which are strong reducing species enough to decompose PFOA [7]. Many other transition metals (than Fe) such as Ag and Co can also be used to activate oxidants in the integrated system [3,4]. In fact, Fe, Co, and Ag are generally the best activators for HP, PMS, and PS, respectively.

When even one of C−F bonds in PFAS is broken by the reductive pathways employing free electrons, hydrogens, and/or more likely SRAs, further decomposition of def-PFAS can be significantly accelerated by the proposed oxidation pathways. Alternatively, the sequence of the reactions is more likely to occur near the functional groups in PFAS. Electron withdrawing groups (i.e., carboxylic acid and sulfonic acid) present in PFOA and PFOS are seemingly impactful on such elemental chemical steps by helping to recruit electrons or radicals to the molecules. Depending on the combinations of oxidants and metals at/in different oxidation states and elemental groups, various reactive species, including but not limited to electrons, hydrogens, and SRAs as reducing species as well as oxidants, HRs, and SRs as oxidizing species, are generated. These species alone or in combination are believed to synergistically decompose and mineralize PFAS. In addition, since PFAS and co-contaminants in IDW have been reported to effectively adsorb onto activated carbon, chemical decomposition of PFAS can also be combined with their physical adsorption (as an option) by embedding the metal particles (M^0/MO_x) into the mesoporous structure of GAC, so-called RAC (GAC/M).

Concept demonstration and its benefits: RAC coupled with oxidants or simply M coupled with oxidants is proposed to implement the ultimate treatment strategy integrating physic adsorption, advanced oxidation, and chemical reduction of PFAS and other co-contaminants, as shown in **Fig. 1**. PFAS are adsorbed onto RAC (i.e., GAC, M^0, and/or MO_x), where M^0 provides electrons and produces hydrogens, while releasing metal ions to activate oxidants for the generation of reactive radicals. This limited scope project tests proof of the concept to determine whether the integrated system is effective to synergistically adsorb and decompose PFAS. In particular, the adsorption-mediated modified Fenton reaction should be quickly evaluated to identify any specific technical challenges involved.

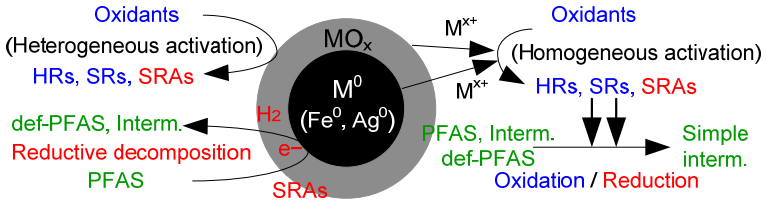

Fig. 1. Generation of reactive species (e.g., e^-, H_2, and SRAs as reducing species and HRs and SRs as oxidizing species) through the Fenton-like reaction between oxidants and transition metal species in the solid/liquid phases, which are involved in the synergistic decomposition of PFAS. Metal particles can also be impregnated into the mesoporous structure of GAC for adsorption of PFAS.

Considering the heterogeneous nature of components in complex media such as IDW and the presence of PFAS and various co-contaminants with different chemical reactivity and affinity, combining multiple treatment technologies (i.e., treatment train approach) is needed to address the chemical stability of PFAS and the real-world complexities of treatment [1]. *For the treatment train approach, we bring up the integrated system, rather than applying associated unit processes in a sequence.*

Materials and Methods

Overall experimental tasks are summarized in **Table 1**. Task 1 on synthesis and characterization of the materials (i.e., Fe^0 and RAC) served as a pre-requisite for other tasks. Task 2, which included main activities in this project, consisted of Steps 1-3. Step 4 dealt with in Task 3 was similar to Step 3, but test media in Step 4 was changed to a mixture of water and soil.

Table 1. Experimental tasks and overview.

Task	Task 2 (Task 1: Synthesis and Characterization)			Task 3
Step	Step 1	**Step 2 (main)**	Step 3	Step 4
Concept	Adsorption	**Decomposition**	Adsorption/Decomposition	Adsorption/Decomposition
Purpose	Can the base GAC adsorb PFAS?	**Can the proposed chemical approach decompose PFAS?**	Can the adsorption-mediated decomposition strategy treat PFAS?	Similar to Step 3 but in water/soil mixture.
Material	GAC	**M/oxidant (e.g., Fe^0/oxidant, Ag^+/oxidant)**	RAC(GAC/M)/oxidant	RAC(GAC/M)/oxidant
Media	Water	**Water**	Water	Water + Soil

Batch experiments: Reactive nanoscale iron particle (RNIP, Toda Kogyo) was purchased and ZVI (boron-coated Fe^0) was home-synthesized [6]. ZVI was impregnated into the mesoporous structure of GAC (Cabot Norit HD3000) [8]. The properties of the materials before and after use were evaluated by using common characterization tools, including visual

morphology, surface area, and particle size. The treatability of GAC, transition metals, and chemical oxidants, alone or in combination under various reaction conditions (i.e., different doses, pHs, and temperatures), was determined in a bench-scale batch reactor containing primarily water and later water and soil mixture [9-12]. The media were spiked with 6 PFAS listed in the United States Environmental Protection Agency's 3rd Uncontrolled Contaminant Monitoring Rule (UCMR-3), i.e., 3 carboxylic PFAS (PFOA, perfluorononanoic acid (PFNA), and perfluoroheptanoic acid (PFHpA)) and 3 sulfonic PFAS (PFOS, perfluorohexanesulfonic acid (PFHxS), and perfluorobutanesulfonic acid (PFBS)). As a polyfluorinated one, 6:2 fluorotelomer sulfonate (6:2 FTS) was also briefly tested. All detailed experimental conditions and chemical concentrations are shown in each figure caption [9-12].

PFAS and chemical analyses: Solid phase extraction followed by liquid chromatograph (LC; Shimadzu Nexera) equipped with a triple quadrupole mass spectrometer (MS; Shimadzu 8040) was used to analyze the target PFAS and expected byproducts such as short chain PFAS (e.g., perfluorohexanoic acid (PFHxA), perfluoropentanoic acid (PFPeA), and perfluorobutanoic acid (PFBA)). Targeted analysis in multiple reaction monitoring scan and negative electrospray ionization was used. Aqueous fluoride ion (F^-) was detected by using an Intellical ISE F121 electrode (Hach) and total organic carbon (TOC) was measured by using TOC analyzer (Shimadzu TOC-V_{csn}). Concentration of PS was traced using a spectrophotometric method on a UV-visible spectrophotometer (Shimadzu 2450). Scavenger tests were conducted with alcohols such as tert-butyl alcohol (TBA) and methanol (MeOH).

Results and Discussion

R1. Adsorption of PFAS onto GAC (Step 1): The affinity of the specific mesoporous GAC (i.e., HD3000) with 6 target PFAS should be evaluated because it is used as a base material to place Fe^0 particles and fabricate RAC for implementing the adsorption-mediated decomposition strategy. Adsorption batch experiments were conducted (**Figs. S1**, **S2**, and **S3** in **Appendix 1. Supporting Data**) [9]. The Langmuir and Freundlich isotherm models were applied, as summarized in **Table 2**. In the Langmuir model, maximum adsorption capacity was ranged from 30.12 mg-PFAS/g-GAC for PFBS to 77.52 mg-PFAS/g-GAC for PFNA. Longer chain PFAS, except for PFOA, were adsorbed more in order of PFNA>PFOS>PFHpA>PFHxS>PFBS, and PFOS as C8 was absorbed more than PFOA. Overall, all PFAS had great affinity for HD3000.

Table 2. Langmuir and Freundlich isotherm parameters for adsorption of PFAS on to GAC.

PFAS	Langmuir Isotherm*			Freundlich Isotherm*		
	Q_m	K_L	r^2	K_F	1/n	r^2
PFNA	77.52	0.26	0.9811	18.11	0.520	0.9954
PFOA	33.11	7.02	0.9170	29.05	0.115	0.6142
PFHpA	58.48	0.05	0.8598	19.77	0.383	0.9354
PFOS	60.24	0.81	0.8997	26.79	0.315	0.9286
PFHxS	47.85	2.40	0.8704	33.20	0.164	0.7481
PFBS	30.12	14.43	0.9344	20.76	0.229	0.8849

* Langmuir isotherm constants Qm (mg PFAS/g GAC) and K_L (L/mg), and Freundlich isotherm constants K_F [(mg PFAS/g GAC)/(mg PFAS/L)$^{1/n}$] and 1/n (PFAS 10 mg/L; GAC 0.025 to 1 g/L; no PS; 20 °C; initial pH 4.5 to final pH around 6.0 (no pH control)).

R2. Decomposition of PFAS by Fe^0/oxidant (Step 2): *Fe^0 or oxidant alone for PFOS:* Prior to its impregnation into GAC, the reactivity of Fe^0 and Fe^0 conjugated oxidants should be proven for chemical decomposition of PFAS. The most challenging PFOS was first tested [10]. Two

tested Fe^0 particles (commercially available RNIP and home-made ZVI) alone were not able to remove PFOS via either reductive defluorination or even physical adsorption (**Fig. S4(a)**) HP, PMS, and PS at temperature of 20-60 ˚C did not show any significant removal of PFOS (**Figs. S4(b)** and **S5**), implying that even heat-activated PS was not effective for PFOS decomposition.

Fe^0 and oxidant for PFOS: Then, Fe^0 was conjugated with oxidants to produce various radicals as shown in **Fig. 2**. PFOS removal was significantly improved upon increase in temperature from 20 ˚C to 60 ˚C. Along with high temperatures, the presence of an oxidant was crucial to expedite PFOS removal. Higher oxidant doses resulted in faster removal of PFOS (**Fig. S6**) and acidic pH was beneficial for PFOS removal in cases of PS and PMS while basic pH was better in case of HP (**Fig. S7**).

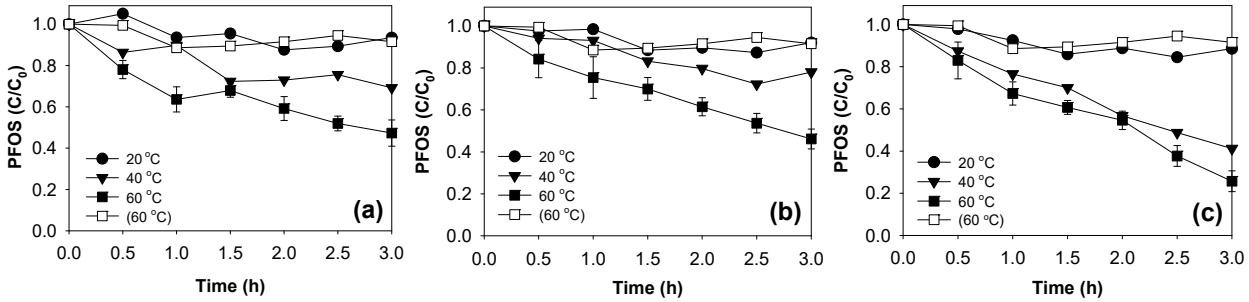

Fig. 2. PFOS removal by Fe^0 conjugated with oxidant (a) PS, (b) PMS, and (c) HP at different temperatures (10 mg/L PFOS; 0.5 g/L Fe^0; 0.3 M PS, 0.3 M PMS or 1.5 M HP; 20-60 °C; initial pH 3 to final pH around 1.5 (no pH control)). (60 °C) indicates the effect of Fe^0 alone (no oxidant) on the removal of PFOS at 60 °C.

Removal mechanisms for PFOS: Since increases in F^- levels and targeted reaction intermediates were not significant in all the cases, only physical removal of PFOS onto Fe^0-associated species was considered to explain the observed PFOS removal, raising many possible complex scenarios occurring in the Fe^0-based integrated system. As observed in **Fig. 2**, Fe^0 itself even at high temperature of 60 ˚C did not show significant removal of PFOS. However, corrosion layers of iron oxides or hydroxides formed as a result of Fe^0 oxidation might adsorb PFOS better, which is supported by the fact that both Fe^0 and oxidant at high temperatures were required for PFOS removal, where Fe^0 can oxidize faster [13]. In a supplementary test, solid Fe_2O_3 (Fe^{3+}) removed PFOS better than FeO (Fe^{2+}) in all pH conditions (3, 7, and 9) (**Fig. S8**). Although only a small amount of solid Fe species was present under acidic condition, pH 3 seemed more beneficial to PFOS removal. Dissolved Fe^{3+} and Fe^{2+} ions (in this order) under pH 3 were also proven to remove PFOS probably via complexation mechanism.

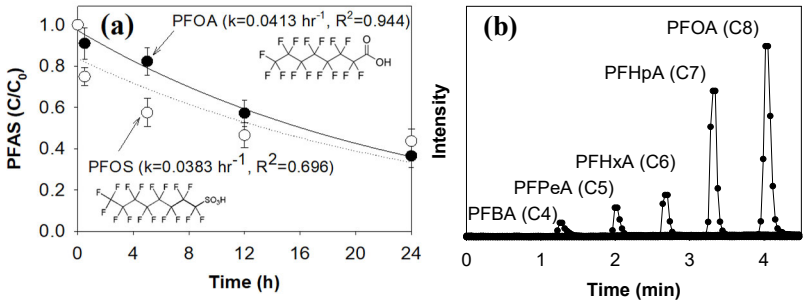

Fig. 3. (a) Removal of PFOS and PFOA by Fe^0 conjugated with PS (10 mg/L PFOA or PFOS; 0.5 g/L Fe^0; 0.3 M PS; 60 °C; initial pH 3 to final pH around 1.5 (no pH control)) and (b) Identification of reaction intermediates formed during PFOA decomposition.

Treatment of PFOA and other PFAS: Since no significant decomposition of PFOS was observed in Fe^0/oxidant system, PFOA, as a counterpart carboxylic PFAS, was quickly tested, as shown in

Fig. 3. PFOA removal was comparable to PFOS removal. Compared to no identifiable intermediates from PFOS, targeted LC/MS analysis indicated formation of several reaction intermediates from PFOA, i.e., short chain PFAS such as PFHpA (C7), PFHxA (C6), PFPeA (C5), and PFBA (C4). Previous studies reported slightly less persistence of PFOA compared to PFOS presumably due to the carboxylic group in PFOA being more vulnerable to chemical reaction than the sulfonic group in PFOS [1,2,5]. Since decomposition of PFOA was obviously observed, other PFAS were tested, as shown in **Fig. 4**. All carboxylic PFAS (PFNA>PFOA>PFHpA) were significantly removed while sulfonic PFAS were slightly removed (PFOS>>PFHxS>PFBS). No identifiable short chain PFAS byproducts were observed for sulfonic PFAS. Meanwhile, decomposition of PFNA (C9) led to formation of PFOA (C8), PFHpA (C7), PFHxA (C6), PFPeA (C5), and PFBA (C4) (**Fig. S9**), suggesting systematic step-by-step removal of CF_2 moieties. Decomposition of PFOA and PFHpA also led to the formation of subsequent short chain PFAS byproducts.

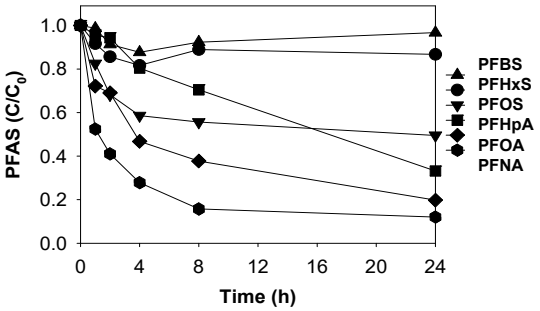

Fig. 4. Removal of various PFAS by Fe^0 conjugated with PS (10 mg/L PFAS; 0.5 g/L Fe^0; 0.3 M PS; 60 °C; initial pH 3 to final pH 1.5 (no pH control)).

R3. Adsorption and decomposition of PFAS by GAC/Fe^0/oxidant (Step 3): Since Steps 1 and 2 showed that GAC adsorbs PFAS and Fe^0/oxidant (particularly PS) decomposes certain PFAS, the adsorption-mediated decomposition of PFAS was attempted by using RAC [9].

RAC characterization: Fe^0 particles were impregnated into GAC. Its surface area was decreased from 593 m^2/g to 336 m^2/g and other characterization results were also comparable to those reported elsewhere [8], implying successful incorporation of 20-30 nm Fe^0 nanoparticles to the mesoporous structure of GAC (**Table S1** and **Fig. S10**).

Performance of RAC: Even in the absence of PS, significant amounts of all PFAS tested were removed (**Fig. S11**). Higher temperature and longer chain PFAS were favorable to PFAS removal. Since no significant reaction byproducts or F^- were detected, the removal can be explained by adsorption mechanisms to Fe^0 and its solid derivatives, as explained above.

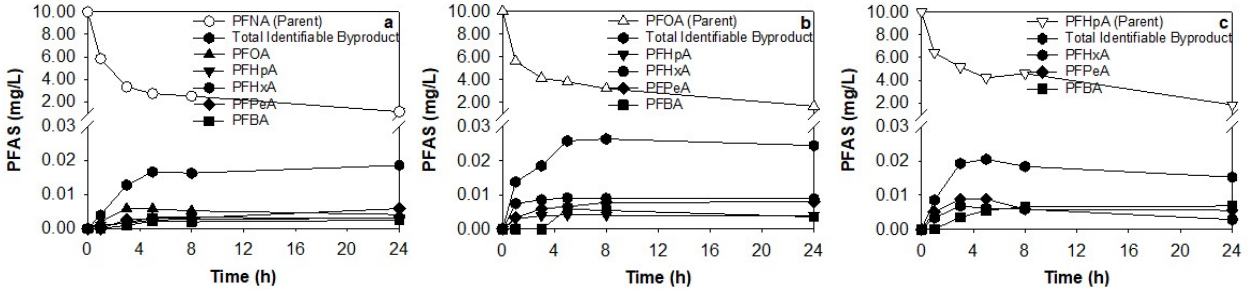

Fig. 5. Evolution of identifiable aqueous byproducts formed during decomposition of PFAS: (a) PFNA, (b) PFOA, and (c) PFHpA in water by RAC conjugated with PS at 60 °C (10 mg/L PFAS; 20 g/L RAC (GAC/Fe^0); 0.3 M PS; 60 °C; initial pH 9 to final pH around 2 (no pH control)).

Performance of RAC and PS: Then, PS was added to RAC (**Fig. S12**). General PFAS removal trends on RAC were the same regardless of the presence of PS. Again, two very similar conclusions were made with respect to decomposition of PFAS; i) only carboxylic PFAS were decomposed, obviously producing short chain PFAS byproduct, as shown in **Fig. 5** (also note **Fig. S13**) and ii) at least around 60 °C was needed to decompose PFAS. Low levels of F^- were

also detected at around 0.01-0.20 mg/L after 24 h. Carboxylic PFAS were removed via physical adsorption combined with chemical decomposition while sulfonic PFAS were removed solely via adsorption mechanism.

R4. Treatment of PFAS in water/soil mixture by GAC/Fe^0/oxidant (Step 4): *Impact of soil:* Removal of PFAS in water and soil slurry was examined (**Figs. S14** and **S15**) [9]. Similar results to those obtained with water were found. Removal was marginally improved in water and soil slurry probably due to the presence of more sorbent materials. F^- was found at 0.01-0.10 mg/L, slightly less than that observed in the case of water. Overall, the presence of soil components seemed not to significantly hinder PFAS removal.

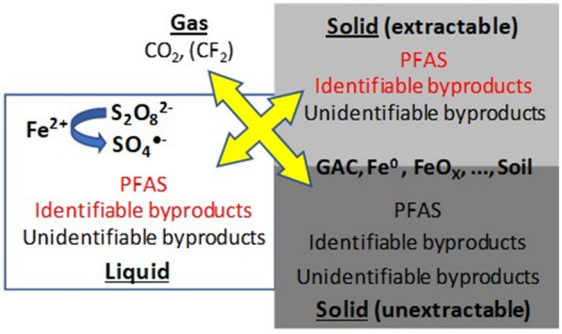

Fig. 6. Partitioning of PFAS and byproducts into the liquid, solid, and gas phases. Carbon mass balance can be set only based on observed PFAS and byproducts (highlighted with red). Please note the number of identifiable byproducts (a few to several) is overwhelmed by that of unidentifiable byproducts.

Partitioning of PFAS and byproducts and mass balance: As depicted in **Fig. 6**, PFAS are adsorbed and partitioned into the aqueous phase, RAC phase, and/or soil phase, and then, if any, they are decomposed to produce various byproducts, which are also re-partitioned into the three phases [14]. Some of PFAS and byproducts may volatilize and undergo mineralization to H_2O and CO_2. However, it is impossible to qualify and quantify all byproducts and recover all PFAS and byproducts from the solid phases. Based on solely the observed results, partitioning of parent PFAS and identifiable byproducts to the aqueous phase and solid phase is summarized in **Fig. 7**.

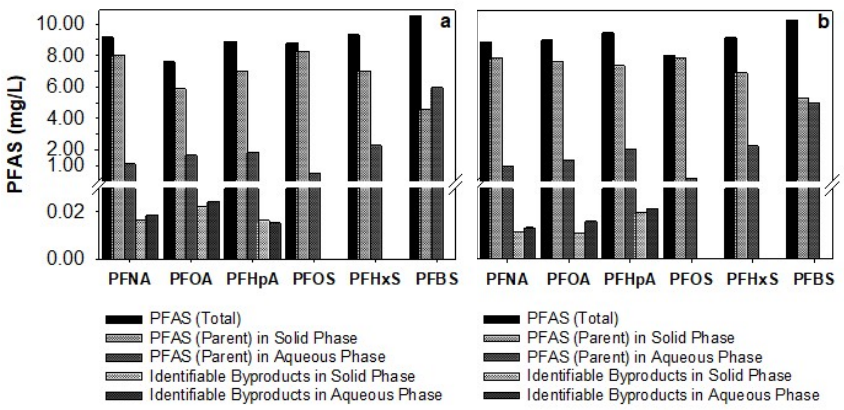

Fig. 7. Partitioning of parent PFAS and identifiable byproducts to the aqueous phase and solid phase after 24 h reaction of PFAS in (a) water and (b) water and soil slurry with RAC conjugated with PS at 60 °C (10 mg/L PFAS; 20 g/L RAC (GAC/Fe^0); no soil and 20g/L soil, 0.3 M PS; 60 °C; initial pH around 9 to final pH around 2 (no pH control)). Solid means RAC for (a) and RAC/soil for (b). Total PFAS represents the sum of all detected parent and byproduct PFAS, in comparison to initial PFAS at 10 mg/L.

Total PFAS observed was slightly less than initial PFAS at 10 m/L (0-24% less). The difference can be considered as unrecovered PFAS, which is ascribed to formation of ill-defined byproducts which were unidentifiable through the targeted analysis used in this study, presence of unextractable parent and byproduct PFAS from the solid phase, and mineralization of PFAS to CO_2. Nonetheless, PFAS were well removed, while staying adsorbed onto the solid phase and waiting for further reaction to be decomposed.

R5. Decomposition of PFAS by metal/oxidant (Ag^+/PS) under ambient conditions (Step 2): In R2-R4, high temperature of at least 40-60 °C was required to decompose carboxylic PFAS by using Fe^0/PS system. We also confirmed that the established heat-activated PS system needs around 60-80 °C for decomposition of PFOA (**Fig. S16**). Short chain byproducts and F^- were detected. However, PFOS was not decomposed by PS even at 80 °C.

Activation of PS using other metals: Since oxidants can also be activated by many other transition metals than Fe exclusively used in R2-R4, we quickly compared Fe^{2+}, Co^{2+}, and Ag^+ for decomposition of PFOA by PS at 20 °C, as shown in **Fig. 8(a)** [11]. Interestingly PS/Ag^+ pair showed noticeable decomposition of PFOA. In general, Ag is the best activator for PS to generate SRs [3]. Since PS was quickly consumed in PS/Ag system (0.15 M to 0.03 M in 48 h, 80% consumption, while only 13% consumption in PS/Fe and PS/Co systems) (**Fig. S17**), adding enough amounts of PS was confirmed to show faster decomposition of PFOA (**Table S2**). Interestingly, the solution color changed from colorless to black followed by eventually colorless due to changes in the speciation of Ag, proposing possible formation of Ag in higher oxidation states at some points (**Fig. S18**). Scavenger tests suggested that both SRs and HRs play a significant role in decomposing PFOA. More experiments employing other transition metals at/in different oxidation states/groups, including gold (Au), nickel (Ni), copper (Cu), and iridium (Ir), should be conducted and the tests in R2-R4 should also be revisited with Ag^0 instead of Fe^0.

Decomposition of various PFAS: Decomposition of one sulfonic PFAS (i.e., PFOS) and three carboxylic PFAS by PS/Ag at 20 °C was compared, as shown in **Fig. 8(b)**. Decomposition of PFOS was not observed while all carboxylic PFAS (PFNA>PFOA>PFHpA) were decomposed significantly. This could be explained most probably by the selectivity of PS/Ag system to attack the carboxylic group in PFAS via Ag-catalyzed oxidative de-carboxylation [15]. As shown in **Fig. 8(c)** (also note **Table S2**), PFNA showed highest defluorination at 20.1%, followed by PFOA at 4.7% and PFHpA at 1.8%. As previously observed in R2-R4, similar short chain PFAS were also detected (**Fig. S19**).

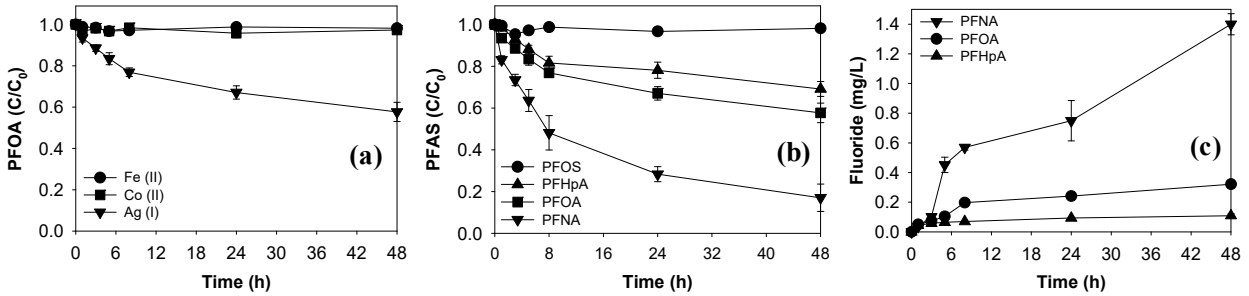

Fig. 8. (a) Decomposition of PFOA by PS conjugated with various transition metals, (b) Decomposition of various PFAS by PS conjugated with Ag^+, and (c) Evolution of F^- released during the decomposition of carboxylic PFAS by PS conjugated with Ag^+ **at room temperature** (10 mg/L PFAS; 0.6 mM metal; 0.15 M PS; **20 °C**; initial pH 4.5 to final pH around 1.5 (no pH control)). Maximum F^- concentration can reach 7.0, 6.9, and 6.8 mg/L for PFNA, PFOA, and PFHpA, respectively.

R6. Decomposition of 6:2 FTS by oxidant (PS) under ambient conditions (Step 2): Since carboxylic PFAS were well decomposed by oxidant/metal systems under ambient conditions in R5, we extended the concept to treating 6:2 FTS as a polyfluorinated one, which is more vulnerable to radical attack than perfluorinated ones [12]. As shown in **Fig. 9**, even oxidants alone at room temperature, particularly PS, were able to decompose 6:2 FTS significantly (its mineralization as TOC reduction was at around 8% for 8 h). Higher PS dose from 0.03 to 0.30 M

(**Fig. S20**) and neutral pH (6.5>>10>3) (**Fig. S21**) were beneficial to 6:2 FTS decomposition. Results on addition of Fe^{2+} as an oxidant activator (**Fig. S22**) and MeOH and TBA as radical scavengers to oxidants (**Fig. S23**) indicated that 6:2 FTS is decomposed via radical mechanisms by both SRs and HRs. Hydrogens in 6:2 FTS were readily available for abstraction reaction by HRs. Meanwhile, abstraction of electrons by SRs from oxygen in the sulfonic group was speculated to occur, resulting in subsequent decomposition of 6:2 FTS (**Fig. S24**).

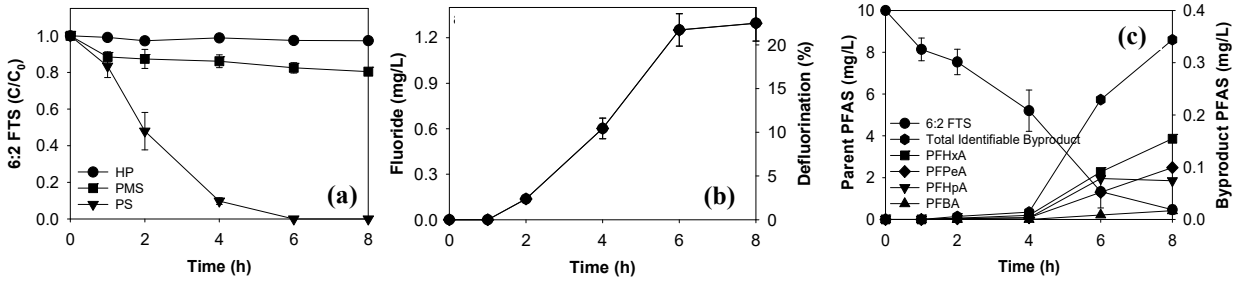

Fig. 9 (a) Decomposition of 6:2 FTS by various oxidants at room temperature and (b-c) Evolution of fluoride ions and reaction byproducts produced during decomposition of 6:2 FTS by PS (10 mg/L 6:2 FTS; 0.3 M oxidant; 20 °C; constant pH at around 6.5 (no pH control)).

Conclusions and Implications for Future Research

This limited scope project successfully demonstrated the potential of the integrated system, i.e., RAC/oxidant or simply M/oxidant, for the synergistic removal and/or decomposition of 6 PFAS (all perfluorinated ones) listed in the UCMR-3. In case of Fe^0, both chemical oxidant and high temperature were required for fast PFAS removal via adsorption and/or decomposition mechanisms. Carbon mass balance suggested that PFAS decomposition and Fe^0 oxidation by radical mechanisms influence, mutually in a complex manner, PFAS adsorption event to GAC, Fe^0 and its derivatives, and soil particles. The most significant learning is that common oxidants conjugated with transition metals (e.g., PS/Ag pair, so-called modified Fenton system) were able to decompose PFAS, particularly carboxylic PFAS, under ambient conditions without introducing any extra energy-intensive tools. However, sulfonic PFAS were removed mainly via adsorption mechanism, while remaining undecomposed under the limited test conditions. As a polyfluorinated one, 6:2 FTS was also decomposed significantly even by PS alone at room temperature. By pairing other oxidants and transition metals at/in different oxidation states/elemental groups, the Fenton reaction (one of the most established, destructive, and practical AOTs) and its modifications should be revisited to better address the issue on treatment of complex media contaminated with PFAS.

As a result, this limited scope study made us <u>one step-closer</u> to establishing our overall objective and study target, i.e., integrated destructive system based on practical technologies as a new research direction. Knowledge obtained from this study could be expanded to treat many other problematic halogenated chemicals (e.g., short-chain PFAS) found in various real-world complex media. If successful, IDW and other complex media containing PFAS can be simply mixed with RAC/oxidants or M/oxidants for their treatment under ambient conditions. Based on the learnings, the following objectives and tasks have been set up for a follow up 3-year project.

<u>Objective I.</u> <u>Accelerating decomposition of PFAS using the promising Fenton-like system.</u>
Task 1: Pairing other common oxidants and transition metals (e.g., Au, Ni, Cu, and Ir) at/in different oxidation states/elemental groups (e.g., Ag^0 and Ag^0/Fe^0) and modifying the Fenton-like system such as intermittent injection of smaller amounts of oxidants.

Task 2: Tackling sulfonic PFAS by exploiting Ag-PS complex such as bis(bipyridine)silver(II) peroxydisulfate known to attack sulfonate [16], catalytic substitution of the hydroxyl group in PFAS with other halogens, and catalytic generation of excessive amounts of SRAs [17].

Objective II. Revealing reaction mechanisms and testing other PFAS using the system.

Task 3: Revealing detailed reaction mechanisms and pathways to answer why and why not in a whole picture of what works (e.g., PS/Ag) and what does not.

Task 4: Testing many PFAS other than those tested in this study, including short chain PFAS and PFAS with different functional groups (e.g., GenX and fluorotelomers).

Objective III. Evaluating real-world utilization of the adsorption-mediated Fenton system.

Task 5: Investigating interaction of the system with real-world environments to reveal fate and transport of PFAS during treatment of an actual IDW containing PFAS.

Task 6: Considering post-treatment issues, including secondary environmental impacts of the materials used and thus disposal and recovery of GAC, transition metals, and inorganic ions.

Literature Cited

[1] N. Merino, et al., Degrading and removal methods for perfluoroalkyl and polyfluoroalkyl substances in water. *Environ. Eng. Sci.* 33 (2016) 615.

[2] C. Vecitis, et al., Treatment technologies for aqueous PFOS and PFOA. *Front. Environ. Sci. Eng. China* 3 (2009) 129.

[3] G. Anipsitakis, D.D. Dionysiou. Radical generation by the interaction of transition metals with common oxidants. *Environ. Sci. Technol.* 38 (2004) 3705.

[4] P. Nfodzo, **H. Choi**, Triclosan decomposition by sulfate radicals: effects of oxidant and metal doses. *Chem. Eng. J.* 174 (2011) 629.

[5] L. Yang, et al. Persulfate-based decomposition of perfluorooctanoic acid (PFOA) and perfluorooctane sulfonate (PFOS) in aqueous solution: Review on influence, mechanism and prospective. *J. Hazard. Mater.* 393 (2020) 122405.

[6] Y. Liu, **H. Choi**, et al., Trichloroethene hydrodechlorination in water by highly disordered monometallic nanoiron. *Chem. Mater.* 17 (2005) 5315.

[7] C.K.O da Silva-Rackov, **H. Choi**, et al., Degradation of PFOA by hydrogen peroxide and persulfate activated by iron-modified diatomite. *Appl. Catal. B: Environ.* 192 (2016) 253.

[8] **H. Choi**, et al., Synthesis of reactive nano Fe/Pd bimetallic system-impregnated activated carbon for the simultaneous adsorption and dechlorination of PCBs. *Chem. Mater.* 20 (2008) 3649.

[9] N. Gevaerd de Souza, **J. Jeon**, **H. Choi**, et al., Removal of PFAS in water and water/soil slurry using Fe-modified reactive activated carbon conjugated with persulfate. *Chem. Eng. J.* (Submitted).

[10] A. Parenky, **J. Jeon**, **H. Choi**, et al., Removal of perfluorooctanesulfonic Acid (PFOS) in water by combining zerovalent iron particles with common oxidants. *Environ. Eng. Sci.* (In Press, DOI: 10.1089/ees.2019.0406).

[11] A. Parenky, **J. Jeon**, **H. Choi**, et al., Decomposition of carboxylic PFAS by persulfate activated by silver under ambient conditions. *J. Environ. Eng.* (Submitted).

[12] A. Parenky, **J. Jeon**, **H. Choi**, et al., Room temperature oxidative transformation of 6:2 fluorotelomer sulfonate by persulfate. *Environ. Eng. Sci.* (In Preparation).

[13] **H. Choi**, et al., Effects of ageing and oxidation of palladized iron embedded in activated carbon on the dechlorination of 2-chlorobiphenyl. *Environ. Sci. Technol.* 43 (2009) 4137.

[14] **H. Choi**, et al., Adsorption and simultaneous dechlorination of PCBs by on GAC/Fe/Pd: mechanistic aspects and reactive capping barrier concept. *Environ. Sci. Technol* 43 (2009) 488.

[15] J.M. Anderson, J.K., Kochi, Silver (I)-catalyzed oxidative decarboxylation of acids by peroxydisulfate. the role of silver (II). *J. Am. Chem. Soc*. 6 (1969) 92.

[16] M. Joshaghani, et al., Oxidative transformation of organic compounds using bis(bipyridine)silver(II) peroxydisulfate. *ARKIVOC* 16 (2007) 260.

[17] P. Asgari, **J. Jeon**, et al., Catalytic hydrogen atom transfer from hydrosilanes to vinylarenes for hydrosilylation and polymerization. *Nature Catal.* 2 (2019) 164; W.-B. Liu, et al., Potassium tert-butoxide-catalyzed dehydrogenative C–H silylation of heteroaromatics: a combined experimental and computational mechanistic study. *J. Am. Chem. Soc.* 139 (2017) 6867; A.A.Toutov, et al., Silylation of C-H bonds in aromatic heterocycles by an Earth-abundant metal catalyst. *Nature* 518 (2015) 80.

Appendix 1

Supporting Data

List of Tables

List of Figures

Fig. S9. Evolution of byproduct formation during decomposition of (a) PFNA, (b) PFOA, and (c) PFHpA (10 mg/L PFAS; 0.5 g/L Fe^0; 0.3 M PS; 60 °C; initial pH 3 to final pH around 1.5 (no pH control)).

Fig. S10. SEM image of fresh RAC (GAC/Fe^0) at different magnifications.

Fig. S11. Removal of aqueous (a) carboxylic PFAS and (b) sulfonic PFAS in water by RAC at (1) 20 ℃, (2) 40 ℃, and (3) 60 ℃ (10 mg/L PFAS; 20 g/L RAC (GAC/Fe^0); no PS; 20-60 ℃; initial pH around 9 to final pH around 8 (no pH control)).

Fig. S12. Removal of aqueous (a) carboxylic PFAS and (b) sulfonic PFAS in water by RAC conjugated with PS at (1) 20 ℃, (2) 40 ℃, and (3) 60 ℃ (10 mg/L PFAS; 20 g/L RAC (GAC/Fe^0); 0.3 M PS; 20-60 ℃; initial pH around 9 to final pH around 2 (no pH control)).

Fig. S13. LC/MS chromatogram based on targeted analysis, showing identifiable aqueous byproducts formed during decomposition of parent PFAS: (a) PFNA, (b) PFOA, and (c) PFHpA in water and soil slurry by RAC conjugated with PS at 60 ℃ (10 mg/L PFAS; 20 g/L RAC (GAC/Fe^0); 20 g/L soil, 0.3 M PS; 60 ℃; initial pH around 9 to final pH around 2 (no pH control)).

Fig. S14. Removal of aqueous (a) carboxylic PFAS and (b) sulfonic PFAS in water and soil slurry by RAC conjugated with PS at 60 ℃ (10 mg/L PFAS; 20 g/L RAC (GAC/Fe^0); 20 g/L soil; 0.3 M PS; 60 ℃; initial pH around 9 to final pH around 2 (no pH control)).

Fig. S15. Evolution of identifiable aqueous byproducts formed during decomposition of parent PFAS: (a) PFNA, (b) PFOA, and (c) PFHpA in water and soil slurry by RAC conjugated with PS at 60 ℃ (10 mg/L PFAS; 20 g/L RAC (GAC/Fe^0); 20 g/L soil, 0.3 M PS; 60 ℃; initial pH around 9 to final pH around 2 (no pH control)).

Fig. S16. Decomposition of PFOA by PS alone at different temperatures (10 mg/L PFOA; no metal; 0.15 M PS; 20-80 °C; initial pH 4.5 to final pH around 1.5 (no pH control)).

Fig. S17. Spectrophotometric determination of PS concentration during decomposition of PFOA by PS conjugated with various transition metals at room temperature after 48 h reaction (10 mg/L PFAS; 0.6 mM metal; 0.15 M PS; 20 °C; initial pH 4.5 to final pH around 1.5 (no pH control)). PS concentration was measured based on absorbance of the reaction solution at 400 nm after digestion with potassium iodide and sodium bicarbonate.

Fig. S18. Solution color evolution during decomposition of PFOA by PS conjugated with Ag^+ at room temperature (10 mg/L PFAS; 0.6 mM Ag^+; 0.15 M PS; 20 °C; initial pH 4.5 to final pH around 1.5 (no pH control)). Very similar color changes were also observed for the other 5 PFAS; PFNA, PFHpA, PFOS, PFHxS, and PFBS. Glass vials were used only for color visualization while polypropylene vials were used for actual PFAS decomposition experiments.

Fig. S19. Evolution of reaction byproducts produced during the decomposition of carboxylic PFAS: (a) PFHpA, (b) PFOA, and (c) PFNA by PS conjugated with Ag^+ at room temperature (10 mg/L PFAS; 0.6 mM Ag^+; 0.15 M PS; 20 °C; initial pH 4.5 to final pH around 1.5 (no pH control)).

Fig. S20. Decomposition of 6:2 FTS by PS at different concentrations (10 mg/L 6:2 FTS; 0.0-0.3 M PS; 20 °C*;* constant pH at around 6.5 (no pH control).

Fig. S21. Decomposition of 6:2 FTS by PS under different pHs (10 mg/L 6:2 FTS; 0.3 M PS; 20 °C; constant pH at around 3.0, 6.5, and 10 (buffer used only for pH 3.0 and 10)).

Fig. S22. Decomposition of 6:2 FTS by various oxidants conjugated with Fe (10 mg/L 6:2 FTS; 0.3 M oxidant; 9 mM of Fe^{2+}; 20 °C; initial pH 6.5 to final pH around 1.5 (no pH control)).

Fig. S23. Decomposition of 6:2 FTS by PS in the presence of radical scavengers (MeOH and TBA) (10 mg/L 6:2 FTS; 0.3 M PS; 0.3 M scavenger; 20 °C; constant pH at around 6.5 (no pH control)).

Fig. S24. Proposed reaction pathway for decomposition of 6:2 FTS by PS (10 mg/L 6:2 FTS; 0.3 M PS; 20 °C; constant pH at around 6.5 (no pH control)).

Table S1. Structural properties of GAC and RAC (GAC/Fe^0).

Property	GAC	RAC
Surface area (m^2/g)	593	336
Average pore diameter (nm)	1.39	1.27
Pore volume (cm^3/g)	0.217	0.106

Table S2. Defluorination of carboxylic PFAS under various reaction conditions at room temperature (48 h reaction; 10 mg/L PFAS; 20 ℃; initial pH 4.5 to final pH around 1.5 (no pH control)).

PFAS	PS (M)	Ag^+ (mM)	F^- (mg/L)	Defluorination (%)
PFNA[a]	**0.15**	**0.6**	**1.4**	**20.1**
PFNA	0.3	0.6	1.8	25.9
PFOA[a]	**0.15**	**0.6**	**0.32**	**4.7**
PFOA	0.15	1.2	0.28	4.1
PFOA	0.3	0.6	0.48	7.0
PFOA	0.6	0.6	0.52	7.5
PFHpA[a]	**0.15**	**0.6**	**0.12**	**1.8**
PFHpA	0.3	0.6	0.18	2.6

[a] Standard condition: 0.15 M PS and 0.6 mM Ag^+.

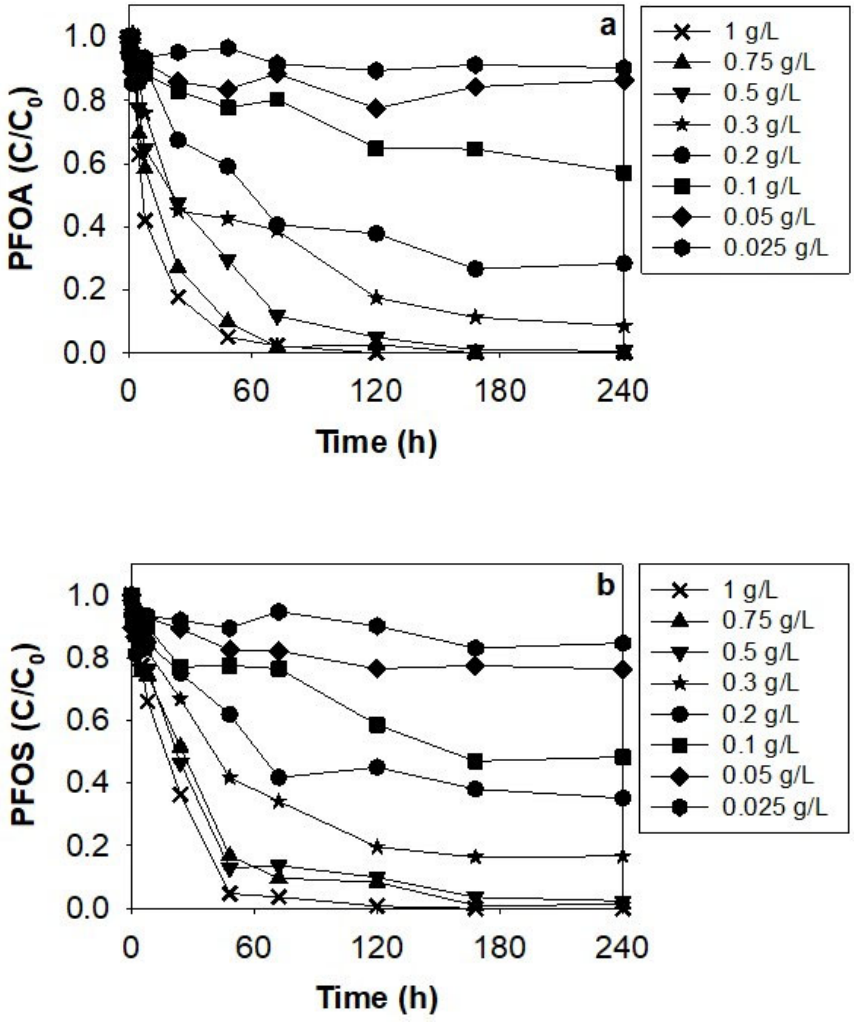

Fig. S1. Removal of aqueous (a) PFOA and (b) PFOS by GAC at various loadings under ambient conditions (PFAS 10 mg/L; GAC 0.025 to 1 g/L; no PS; 20 ℃; initial pH 4.5 to final pH around 6.0 (no pH control)).

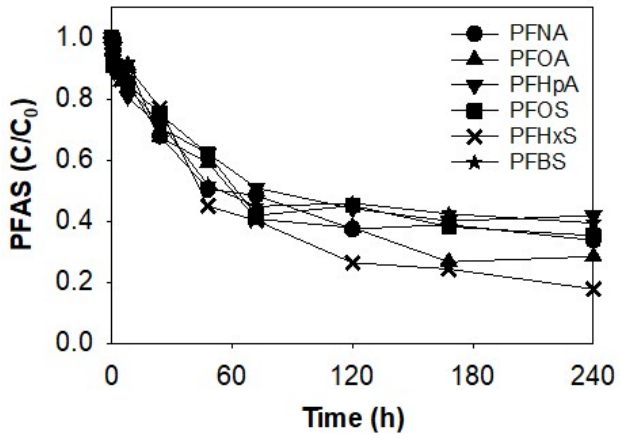

Fig. S2. Removal of various aqueous PFAS by GAC under ambient conditions (PFAS 10 mg/L; GAC 0.2 g/L; no PS; 20 ℃; initial pH 4.5 to final pH around 6.0 (no pH control)).

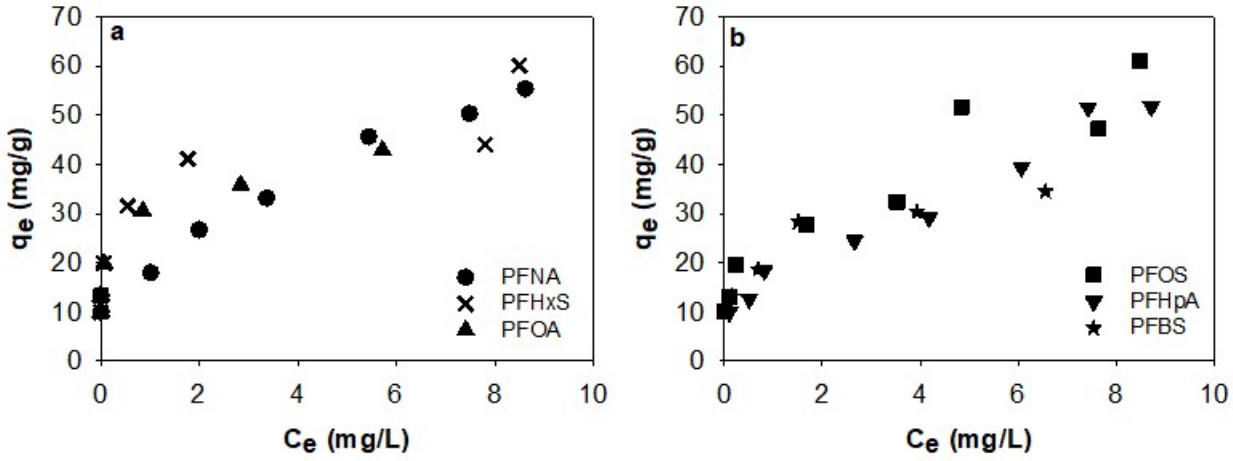

Fig. S3. Adsorption isotherms of (a) PFNA, PFHxS and PFOA and (b) PFOS, PFHpA and PFBS in water onto GAC under ambient conditions (PFAS 10 mg/L; GAC 0.025 to 1 g/L; no PS; 20 °C; initial pH 4.5 to final pH around 6.0 (no pH control)).

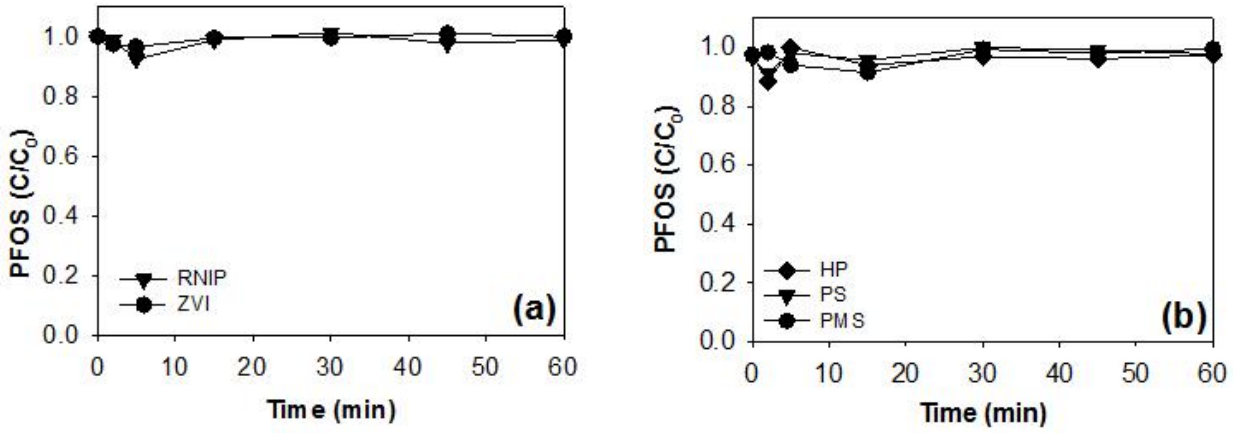

Fig. S4. (a) PFOS removal by Fe^0 (ZVI or RNIP) alone (10 mg/L PFOS; 0.5 g/L Fe^0; no oxidant; 20 °C; initial pH 7 to final pH around 7.2 (no further pH control)) and (b) PFOS removal by oxidant (HP, PS or PMS) alone (10 mg/L PFOS; no Fe^0; 1.5 M HP, 0.3 M PS or 0.3 M PMS; 20 °C; initial pH 7 to final pH around 6.8 (no further pH control)). Note different concentrations for HP, PS, and PMS were used.

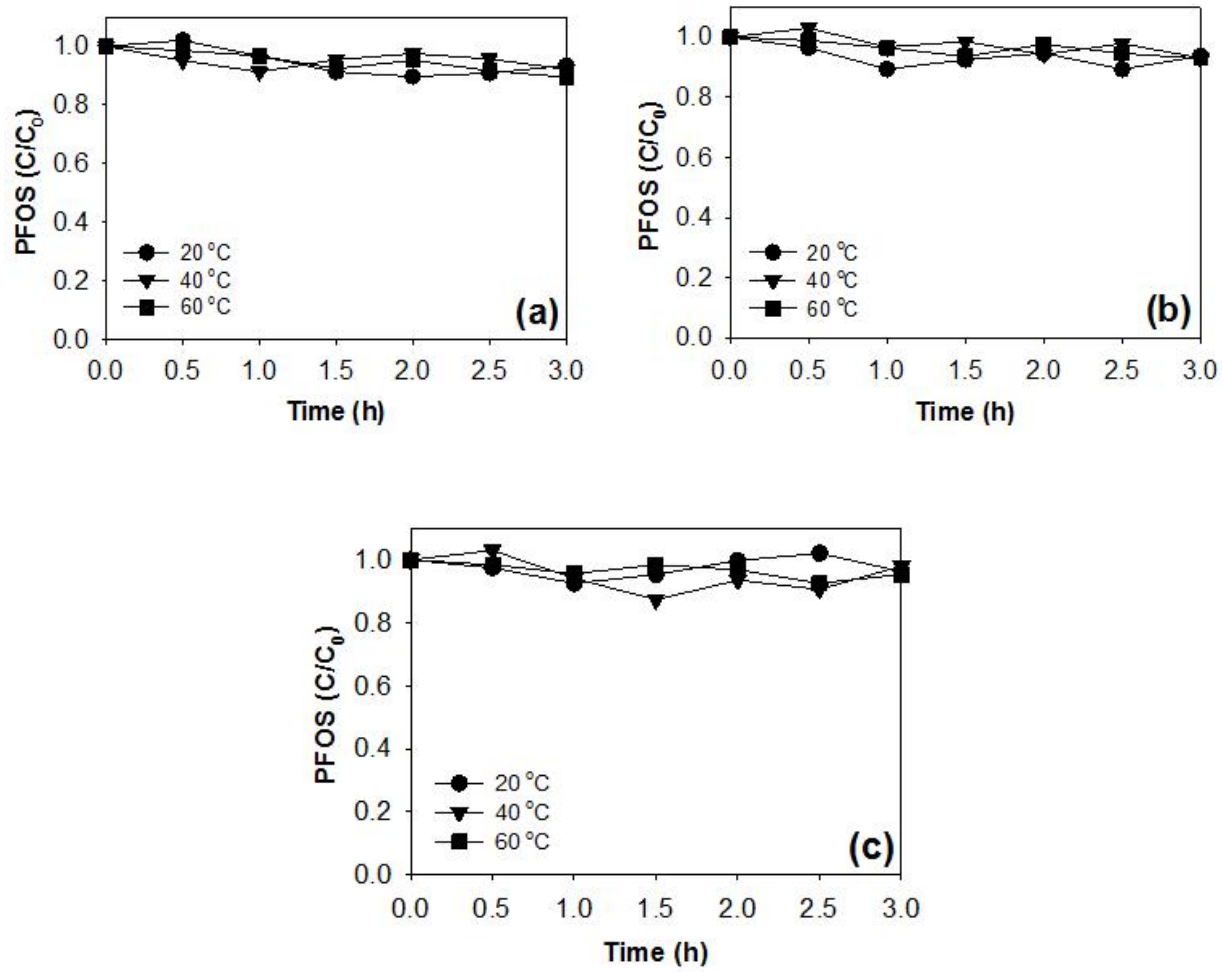

Fig. S5. PFOS removal by oxidants alone (a) PS, (b) PMS, and (c) HP at different temperatures (10 mg/L PFOS; no Fe^0; 0.3 M PS, 0.3 M PMS or 1.5 M HP; 20, 40 or 60 °C; initial pH 3 to final pH around 2 (no pH control)).

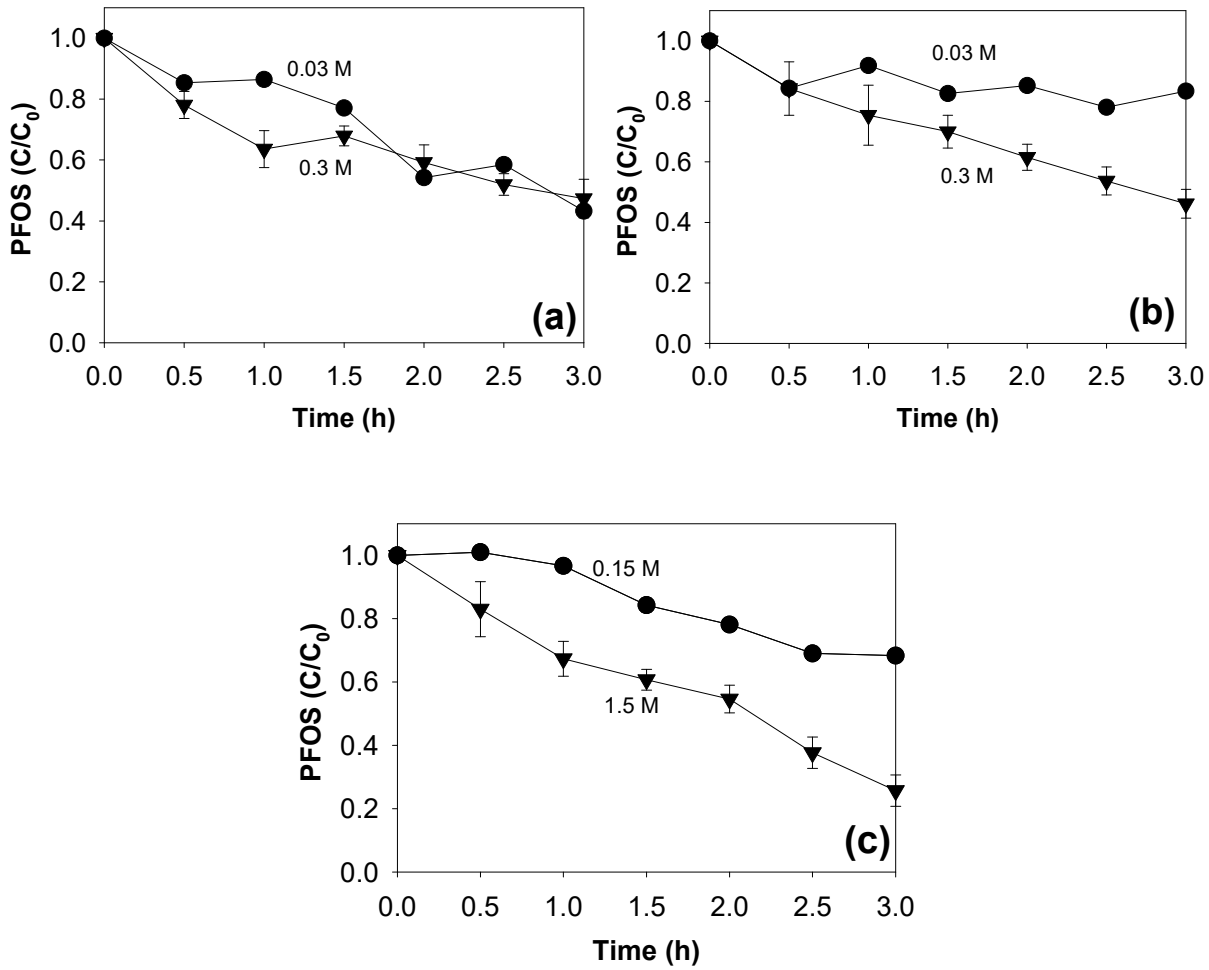

Fig. S6. PFOS removal by Fe^0 conjugated with oxidant (a) PS, (b) PMS, and (c) HP at different concentrations (10 mg/L PFOS; 0.5 g/L Fe^0; 0.03 or 0.3 M PS, 0.03 or 0.3 M PMS, or 0.15 or 1.5 M HP; 60 °C; initial pH 3 to final pH around 1.5 (no pH control)). The error bars are the standard deviation of triplicated results.

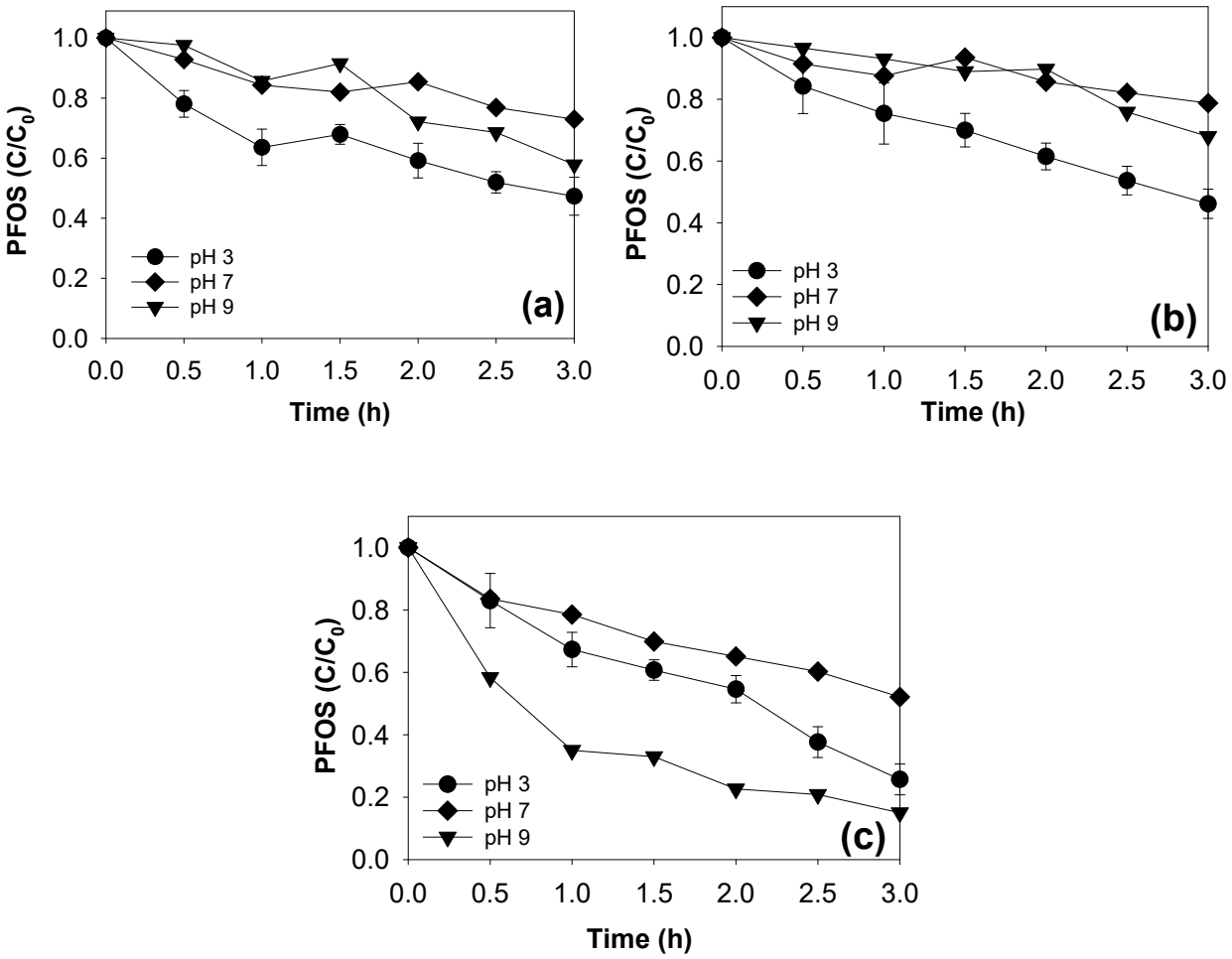

Fig. S7. PFOS removal by Fe^0 conjugated with oxidant (a) PS, (b) PMS, and (c) HP at different initial pH conditions (10 mg/L PFOS; 0.5 g/L Fe^0; 0.3 M PS, 0.3 M PMS, or 1.5 M HP; 60 °C; initial pH 3, 7 or 9 to final pH all around 1.5 (no further pH control)).

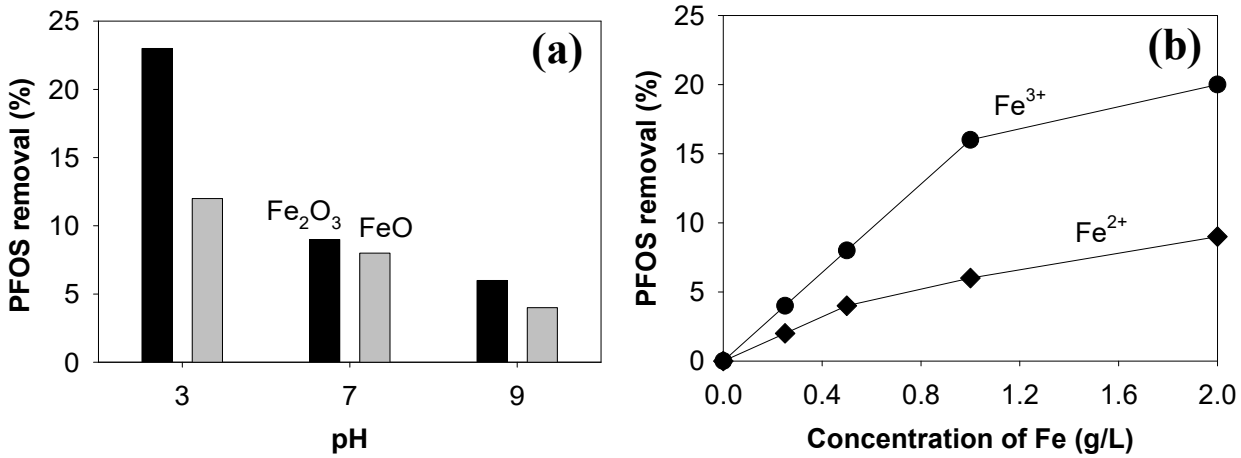

Fig. S8. PFOS removal by (a) adsorption to solid Fe_2O_3 and FeO particles under different initial pH conditions and (b) complexation with dissolved Fe^{3+} and Fe^{2+} ions under different Fe doses (10 mg/L PFOS; 0.5 g/L as Fe; 60 °C; initial pH 3, 7, or 9 to final pH around 3, 7, or 9, respectively (no further pH control) for (a) and 10 mg/L PFOS; 0.25-2 g/L as Fe; 60 °C; initial pH 3 to final pH around 3 (no pH control)for (b)).

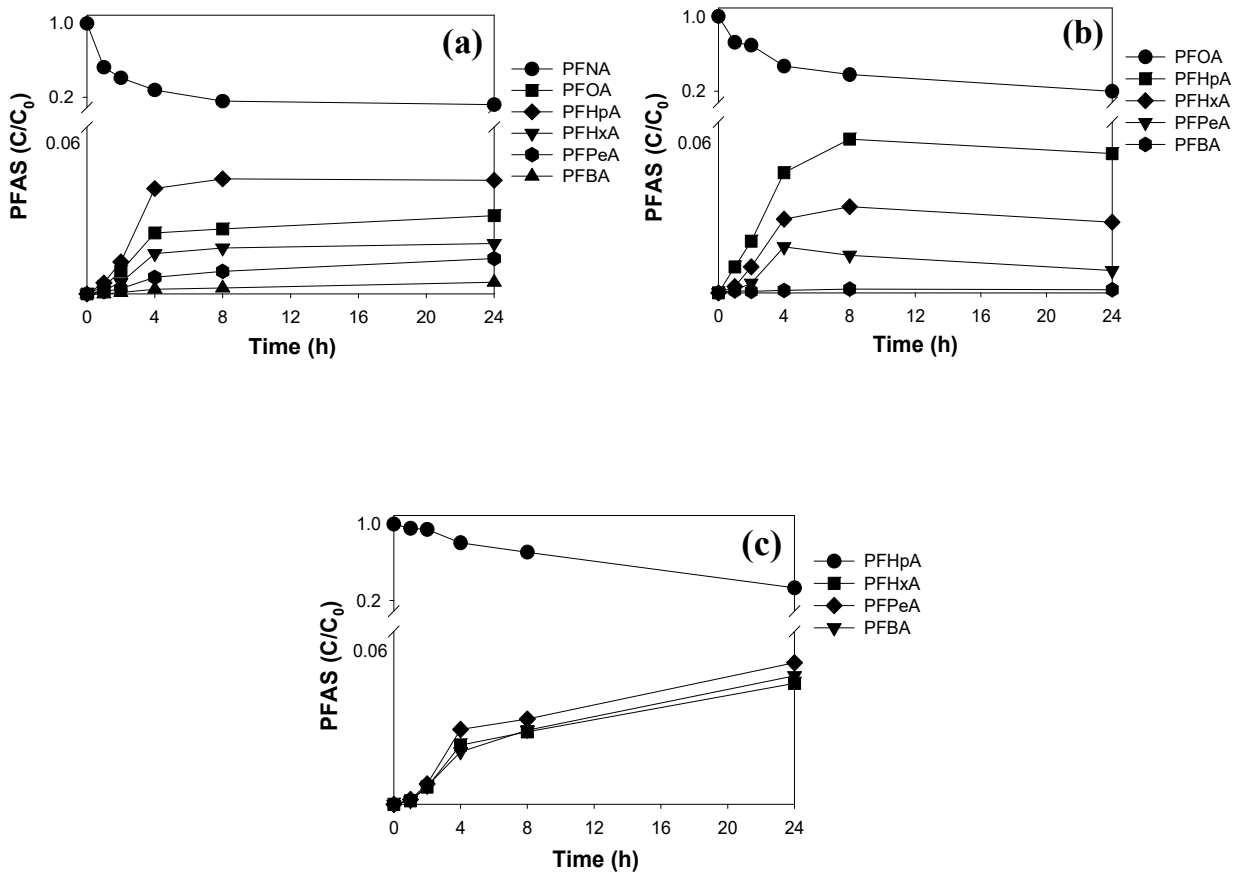

Fig. S9. Evolution of byproduct formation during decomposition of (a) PFNA, (b) PFOA, and (c) PFHpA (10 mg/L PFAS; 0.5 g/L Fe^0; 0.3 M PS; 60 °C; initial pH 3 to final pH around 1.5 (no pH control)).

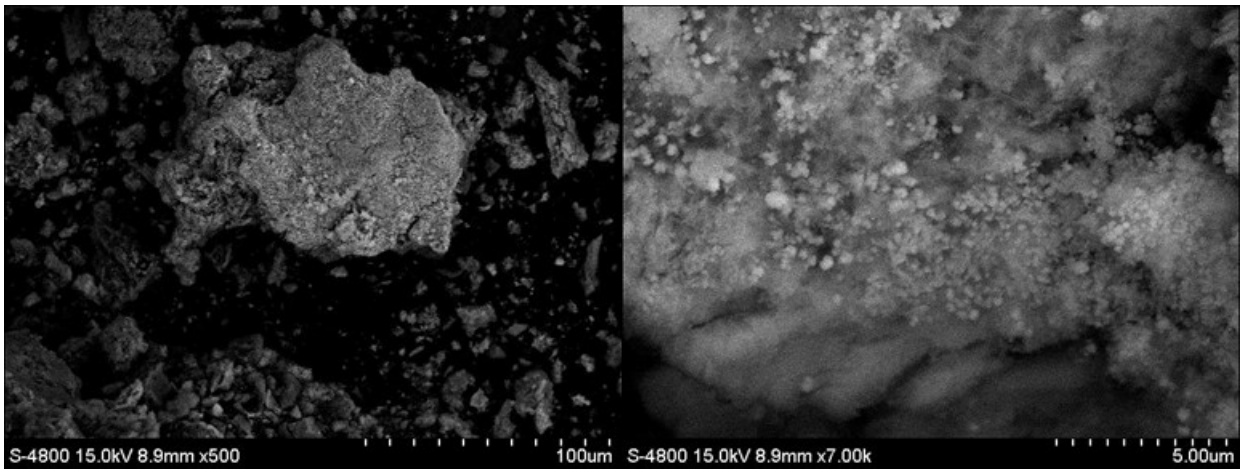

Fig. S10. SEM image of fresh RAC (GAC/F^0) at different magnifications.

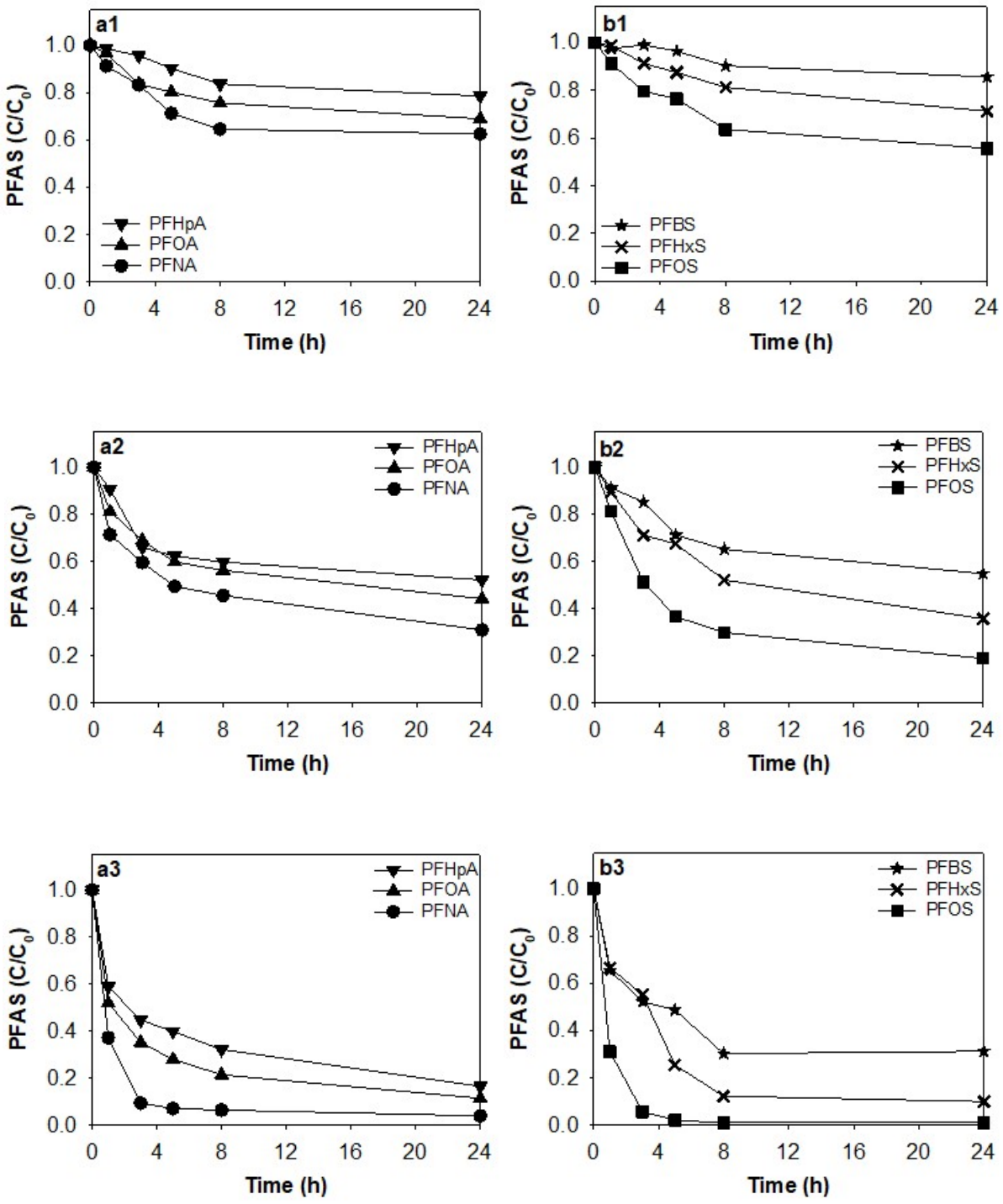

Fig. S11. Removal of aqueous (a) carboxylic PFAS and (b) sulfonic PFAS in water by RAC at (1) 20 ℃, (2) 40 ℃, and (3) 60 ℃ (10 mg/L PFAS; 20 g/L RAC (GAC/Fe^0); no PS; 20-60 ℃; initial pH around 9 to final pH around 8 (no pH control)).

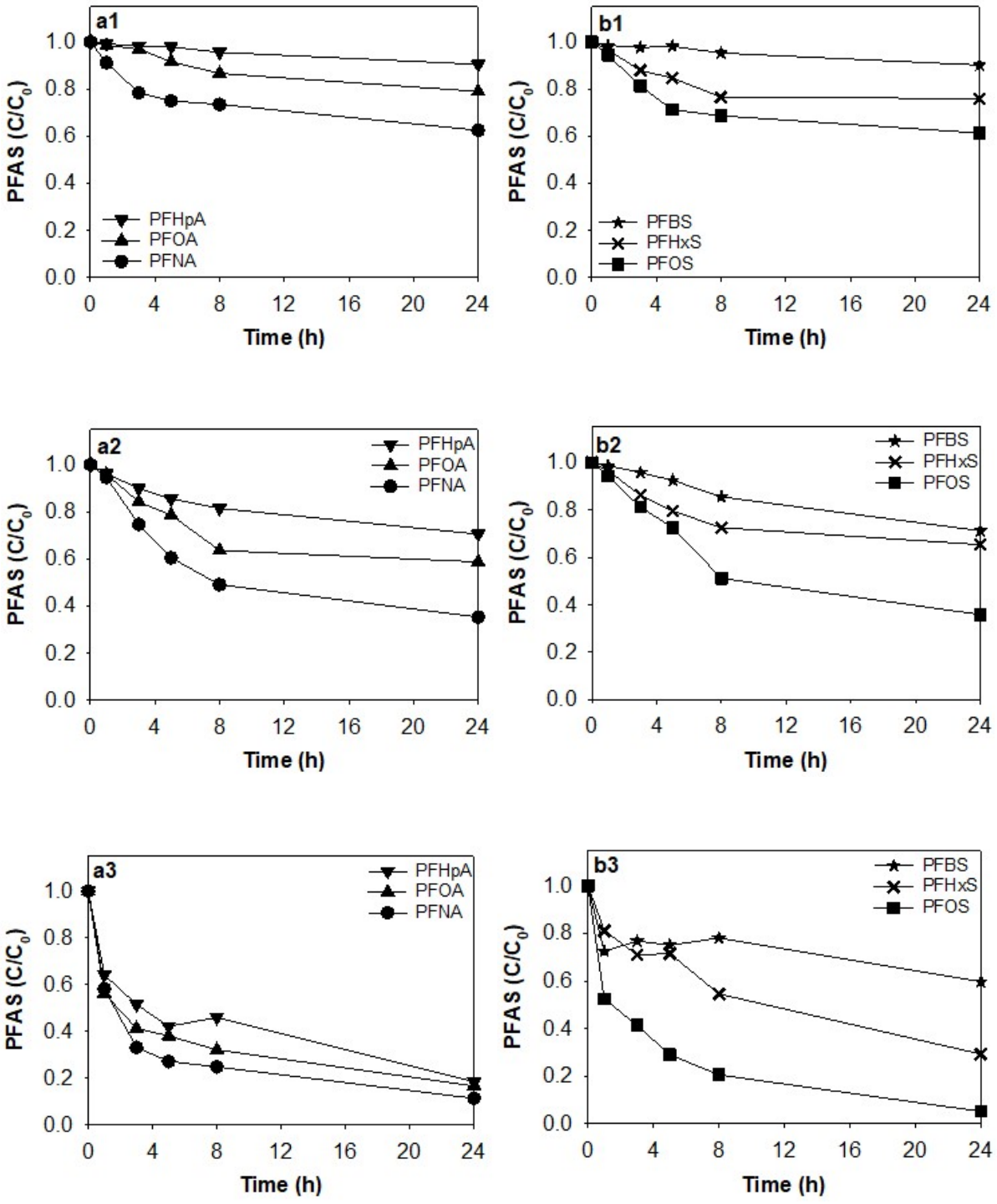

Fig. S12. Removal of aqueous (a) carboxylic PFAS and (b) sulfonic PFAS in water by RAC conjugated with PS at (1) 20 ℃, (2) 40 ℃, and (3) 60 ℃ (10 mg/L PFAS; 20 g/L RAC (GAC/Fe^0); 0.3 M PS; 20-60 ℃; initial pH around 9 to final pH around 2 (no pH control)).

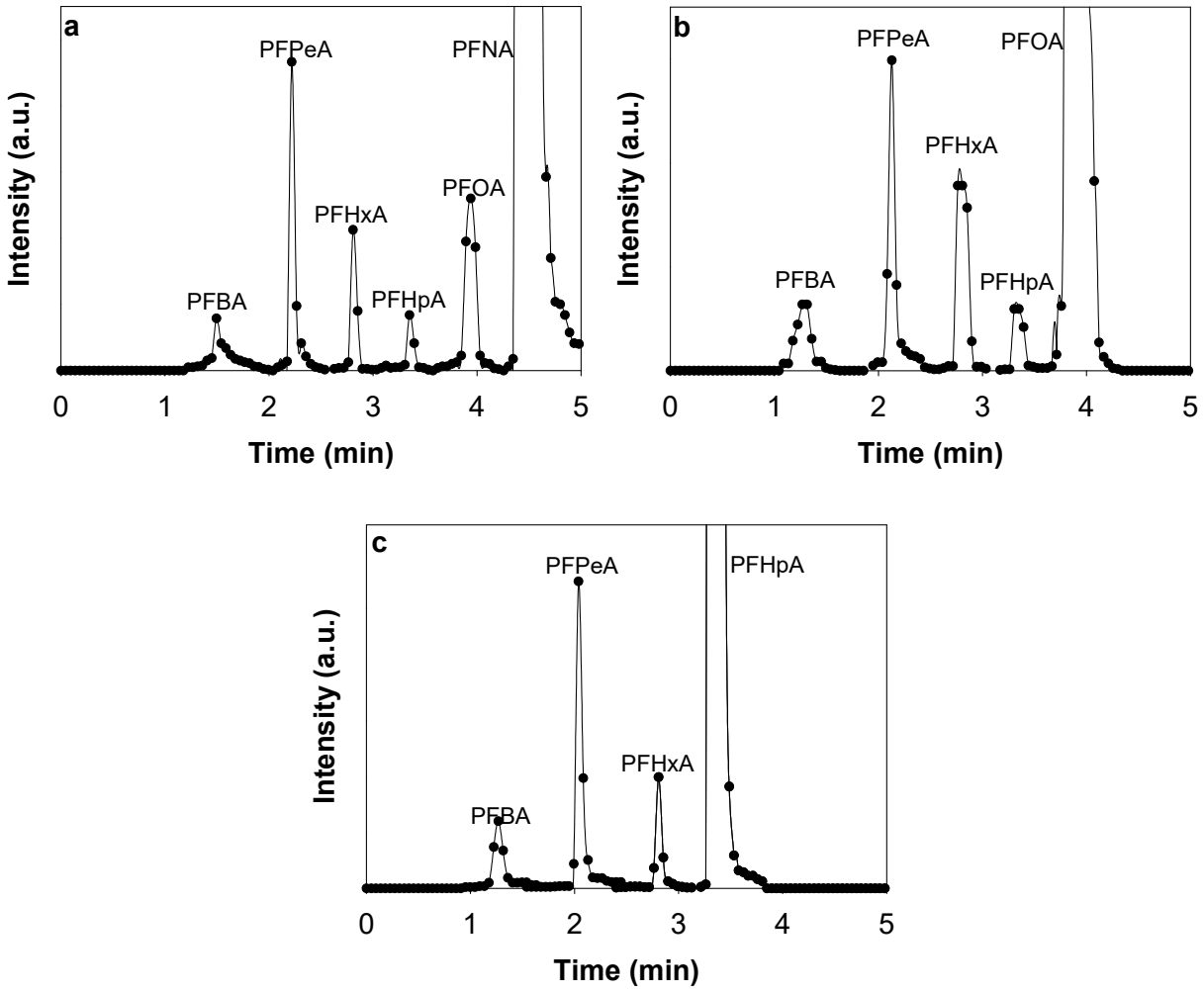

Fig. S13. LC/MS chromatogram based on targeted analysis, showing identifiable aqueous byproducts formed during decomposition of parent PFAS: (a) PFNA, (b) PFOA, and (c) PFHpA in water and soil slurry by RAC conjugated with PS at 60 ℃ (10 mg/L PFAS; 20 g/L RAC (GAC/Fe^0); 20 g/L soil, 0.3 M PS; 60 ℃; initial pH around 9 to final pH around 2 (no pH control)).

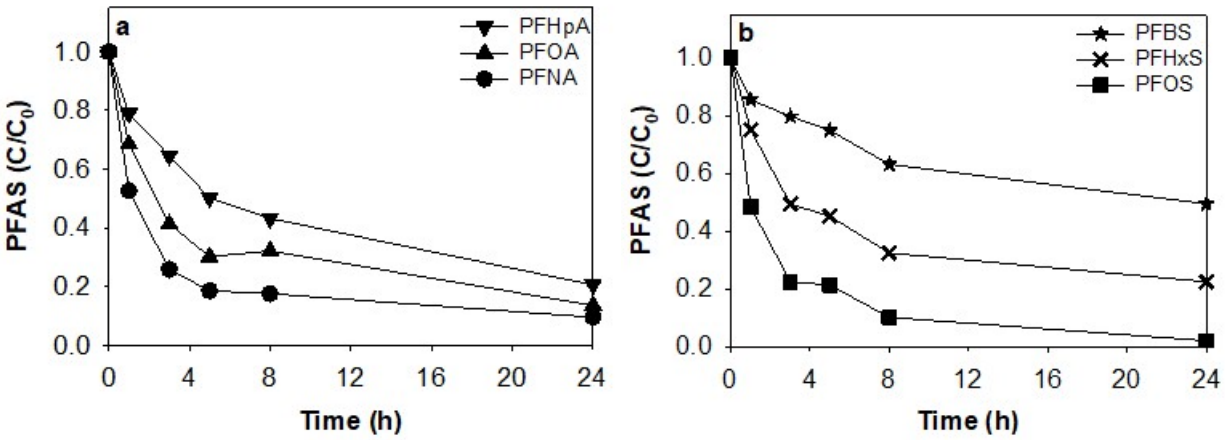

Fig. S14. Removal of aqueous (a) carboxylic PFAS and (b) sulfonic PFAS in water and soil slurry by RAC conjugated with PS at 60 ℃ (10 mg/L PFAS; 20 g/L RAC (GAC/Fe^0); 20 g/L soil; 0.3 M PS; 60 ℃; initial pH around 9 to final pH around 2 (no pH control)).

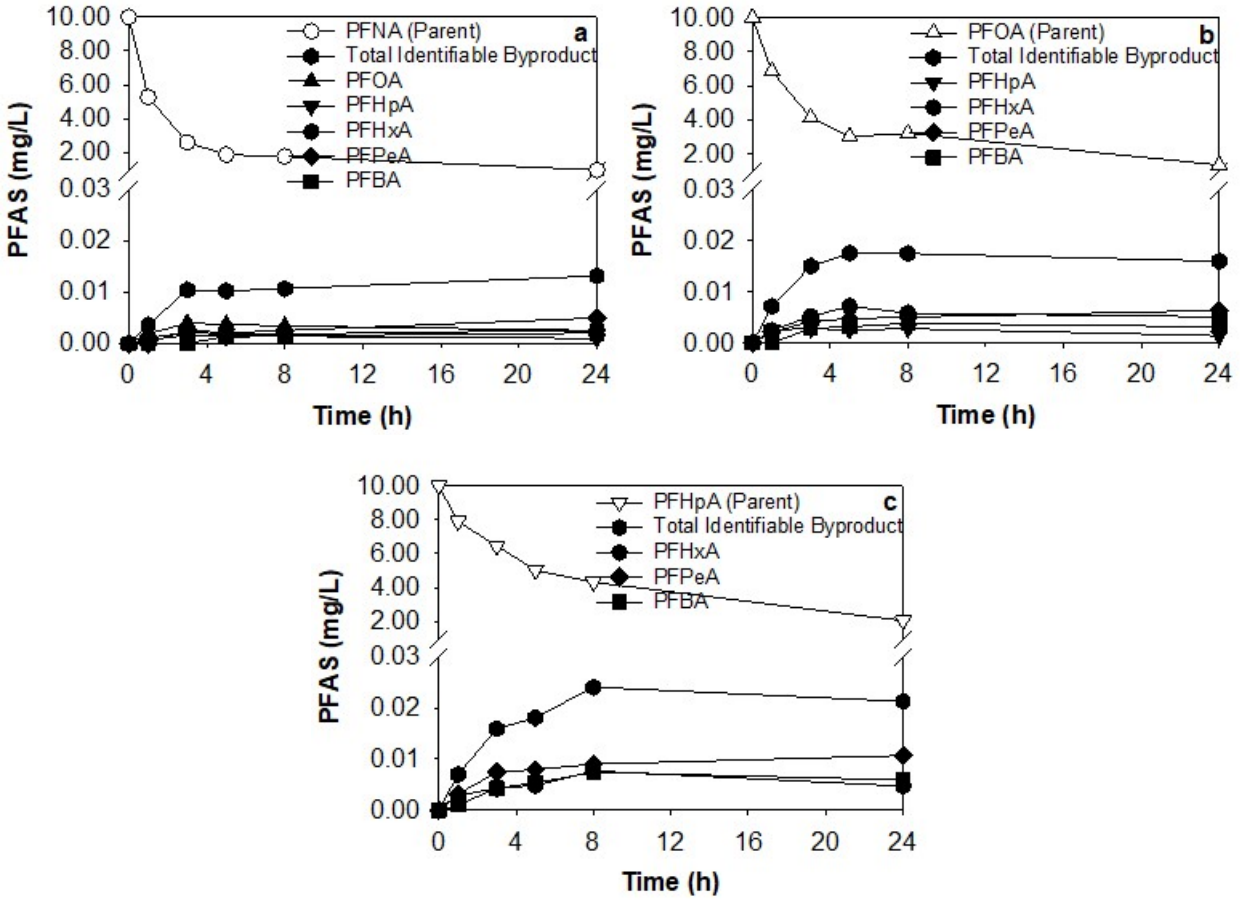

Fig. S15. Evolution of identifiable aqueous byproducts formed during decomposition of parent PFAS: (a) PFNA, (b) PFOA, and (c) PFHpA in water and soil slurry by RAC conjugated with PS at 60 °C (10 mg/L PFAS; 20 g/L RAC (GAC/Fe^0); 20 g/L soil, 0.3 M PS; 60 °C; initial pH around 9 to final pH around 2 (no pH control)).

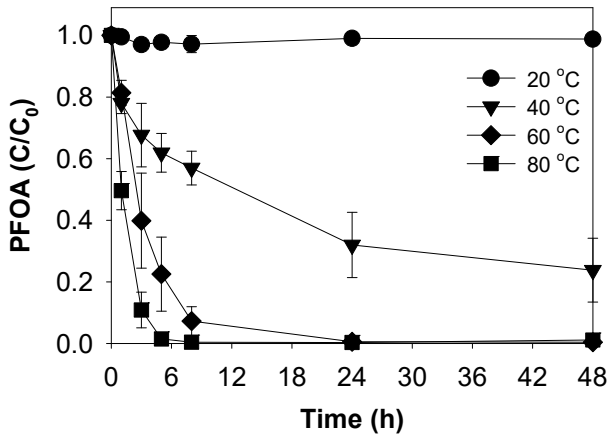

Fig. S16. Decomposition of PFOA by PS alone at different temperatures (10 mg/L PFOA; no metal; 0.15 M PS; 20-80 °C; initial pH 4.5 to final pH around 1.5 (no pH control)).

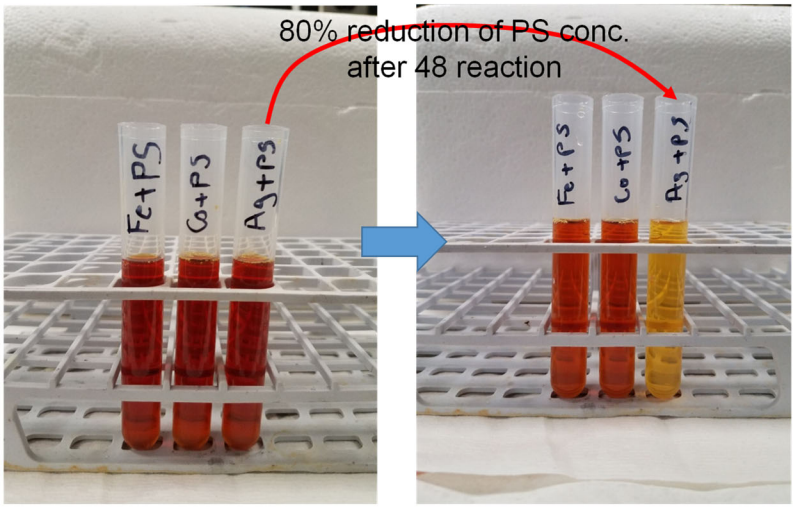

Fig. S17. Spectrophotometric determination of PS concentration during decomposition of PFOA by PS conjugated with various transition metals at room temperature after 48 h reaction (10 mg/L PFAS; 0.6 mM metal; 0.15 M PS; 20 °C; initial pH 4.5 to final pH around 1.5 (no pH control)). PS concentration was measured based on absorbance of the reaction solution at 400 nm after digestion with potassium iodide and sodium bicarbonate.

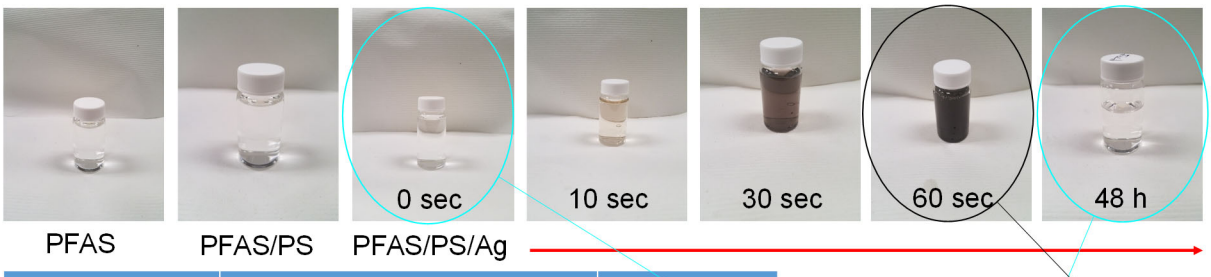

Condition			Reaction Solution Color	PFAS Decomposition
Ag	PS	PFAS		
O	X	X	Colorless	-
O	X	O	Colorless	NO
X	O	X	Colorless	-
X	O	O	Colorless	NO
O	O	X	Colorless → Black → Colorless	-
O	O	O	Colorless → Black → Colorless	YES

$Ag^{+} + S_2O_8^{2-} \rightarrow SO_4^{\bullet-} + SO_4^{-} + Ag^{2+}$ (1)

$Ag^{2+} + SO_4^{\bullet-} \rightarrow Ag^{+} + SO_4^{-}$ (2)

Fig. S18. Solution color evolution during decomposition of PFOA by PS conjugated with Ag^{+} at room temperature (10 mg/L PFAS; 0.6 mM Ag^{+}; 0.15 M PS; 20 °C; initial pH 4.5 to final pH around 1.5 (no pH control)). Very similar color changes were also observed for the other 5 PFAS; PFNA, PFHpA, PFOS, PFHxS, and PFBS. Glass vials were used only for color visualization while polypropylene vials were used for actual PFAS decomposition experiments.

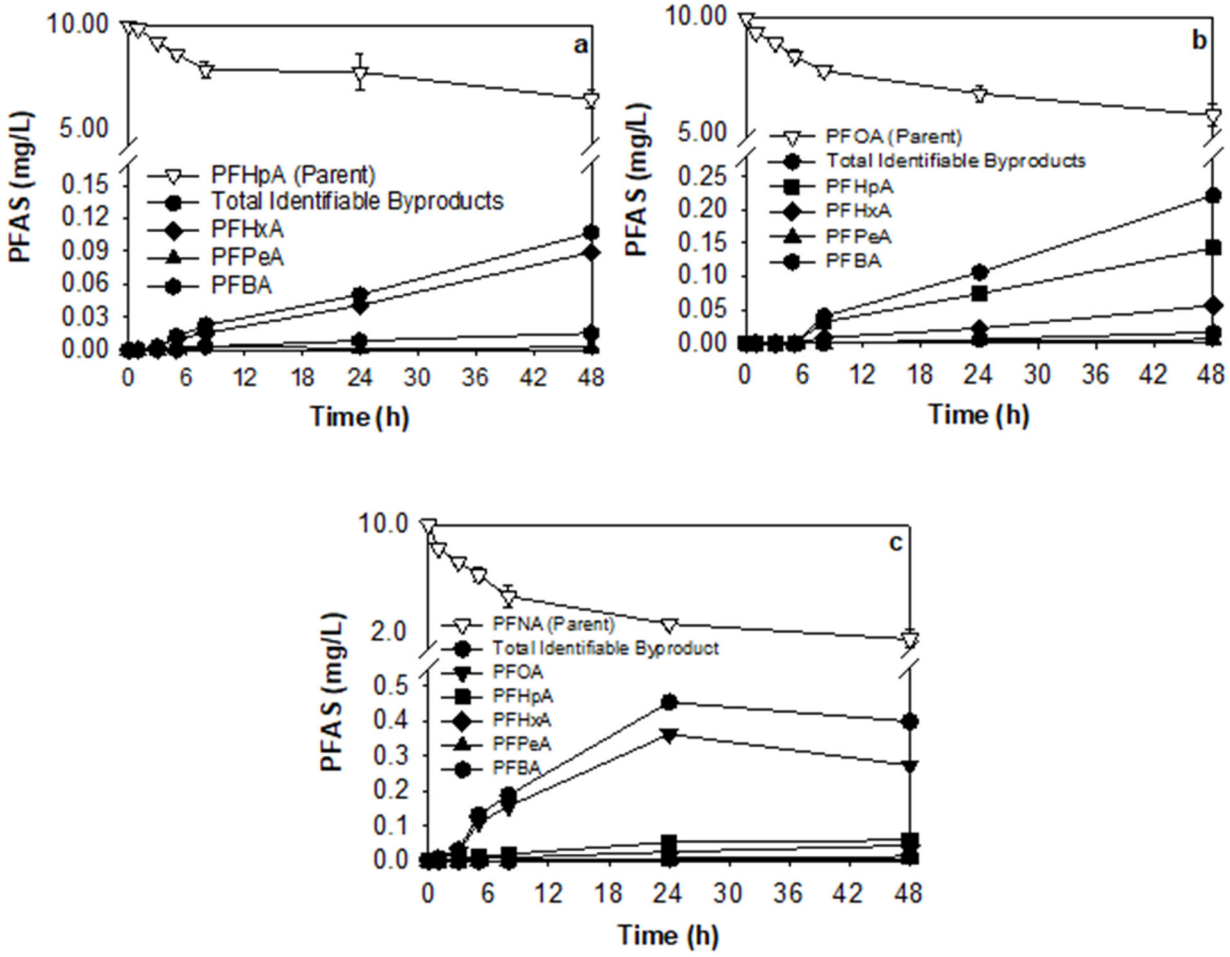

Fig. S19. Evolution of reaction byproducts produced during the decomposition of carboxylic PFAS: (a) PFHpA, (b) PFOA, and (c) PFNA by PS conjugated with Ag^{+} at room temperature (10 mg/L PFAS; 0.6 mM Ag^{+}; 0.15 M PS; 20 °C; initial pH 4.5 to final pH around 1.5 (no pH control)).

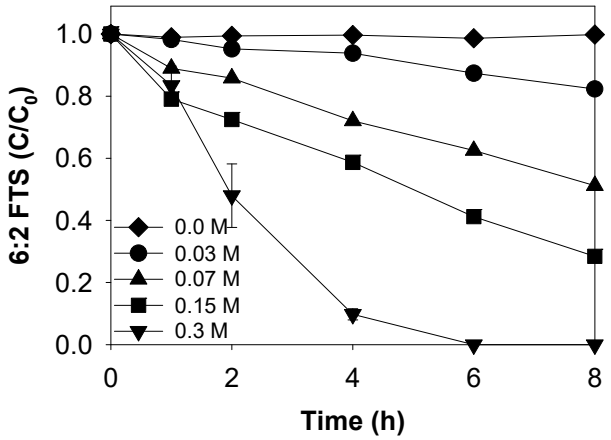

Fig. S20. Decomposition of 6:2 FTS by PS at different concentrations (10 mg/L 6:2 FTS; 0.0-0.3 M PS; 20 °C*;* constant pH at around 6.5 (no pH control).

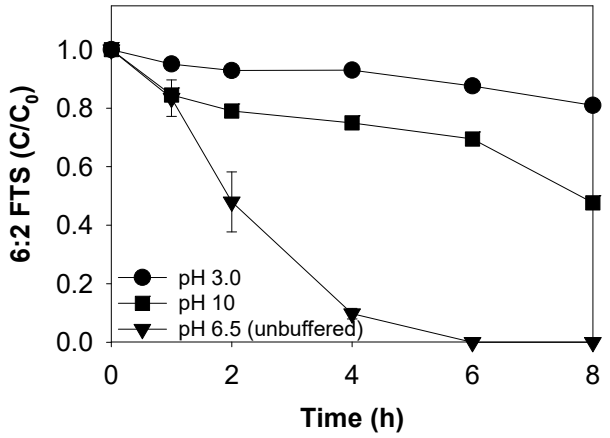

Fig. S21. Decomposition of 6:2 FTS by PS under different pHs (10 mg/L 6:2 FTS; 0.3 M PS; 20 °C; constant pH at around 3.0, 6.5, and 10 (buffer used only for pH 3.0 and 10)).

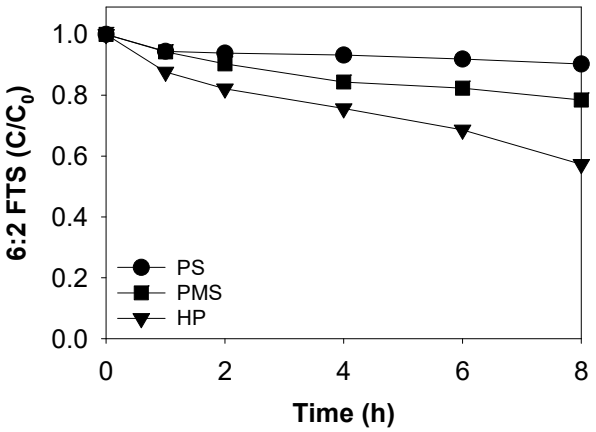

Fig. S22. Decomposition of 6:2 FTS by various oxidants conjugated with Fe (10 mg/L 6:2 FTS; 0.3 M oxidant; 9 mM of Fe^{2+}; 20 °C; initial pH 6.5 to final pH around 1.5 (no pH control)).

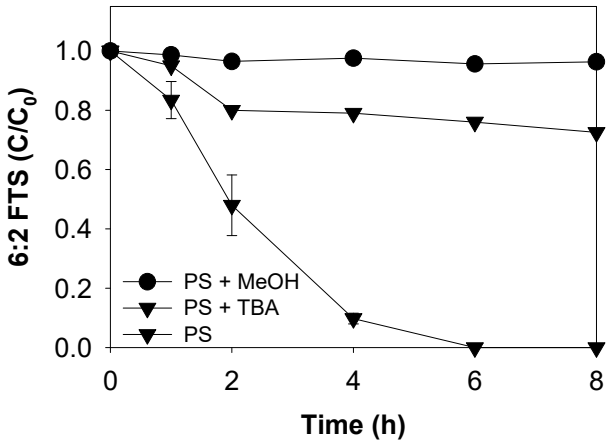

Fig. S23. Decomposition of 6:2 FTS by PS in the presence of radical scavengers (MeOH and TBA) (10 mg/L 6:2 FTS; 0.3 M PS; 0.3 M scavenger; 20 °C; constant pH at around 6.5 (no pH control)).

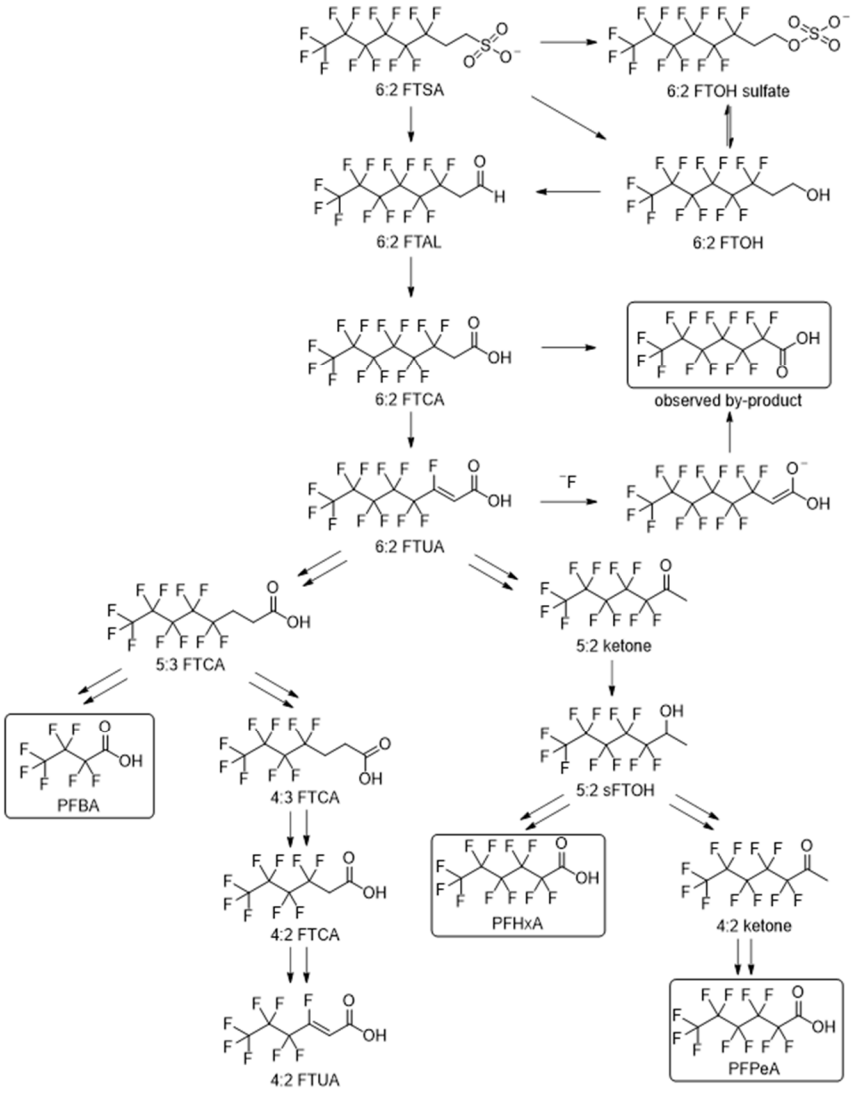

Fig. S24. Proposed reaction pathway for decomposition of 6:2 FTS by PS (10 mg/L 6:2 FTS; 0.3 M PS; 20 °C; constant pH at around 6.5 (no pH control)).